





# **UNIVERSIDAD DE INVESTIGACIÓN DE TECNOLOGÍA EXPERIMENTAL YACHAY TECH**

**Escuela de Ciencias Químicas e Ingeniería**

## **Virtual Modeling and Design of an Optimal Light Emitting Diodes- based Photocatalyst Test System**

Trabajo de integración curricular presentado como requisito  
para la obtención del título de Petroquímico

**Autor:**

Fierro Pita Oscar Alexander

**Tutores:**

Manuel Caetano, Ph.D.

Alex Palma, Ph.D.

Urcuquí, Julio 2021

**SECRETARÍA GENERAL**  
(Vicerrectorado Académico/Cancillería)  
**ESCUELA DE CIENCIAS QUÍMICAS E INGENIERÍA**  
**CARRERA DE PETROQUÍMICA**  
**ACTA DE DEFENSA No. UITEY-CHE-2021-00020-AD**

A los 2 días del mes de julio de 2021, a las 13:00 horas, de manera virtual mediante videoconferencia, y ante el Tribunal Calificador, integrado por los docentes:

<b>Presidente Tribunal de Defensa</b>	Dr. RICAURTE FERNANDEZ, MARVIN JOSE , Ph.D.
<b>Miembro No Tutor</b>	Dr. TAFUR GUISAO, JUAN PABLO , Ph.D.
<b>Tutor</b>	Dr. CAETANO SOUSA MANUEL , Ph.D.

El(la) señor(ita) estudiante **FIERRO PITA, OSCAR ALEXANDER**, con cédula de identidad No. **1004296008**, de la **ESCUELA DE CIENCIAS QUÍMICAS E INGENIERÍA**, de la Carrera de **PETROQUÍMICA**, aprobada por el Consejo de Educación Superior (CES), mediante Resolución **RPC-SO-39-No.456-2014**, realiza a través de videoconferencia, la sustentación de su trabajo de titulación denominado: **VIRTUAL MODELING AND DESIGN OF AN OPTIMAL LIGHT EMITTING DIODES-BASED PHOTOCATALYST TEST SYSTEM**, previa a la obtención del título de **PETROQUÍMICO/A**.

El citado trabajo de titulación, fue debidamente aprobado por el(los) docente(s):

<b>Tutor</b>	Dr. CAETANO SOUSA MANUEL , Ph.D.
<b>Co - Tutor</b>	Dr. PALMA CANDO, ALEX URIEL , Ph.D.

Y recibió las observaciones de los otros miembros del Tribunal Calificador, las mismas que han sido incorporadas por el(la) estudiante.

Previamente cumplidos los requisitos legales y reglamentarios, el trabajo de titulación fue sustentado por el(la) estudiante y examinado por los miembros del Tribunal Calificador. Escuchada la sustentación del trabajo de titulación a través de videoconferencia, que integró la exposición de el(la) estudiante sobre el contenido de la misma y las preguntas formuladas por los miembros del Tribunal, se califica la sustentación del trabajo de titulación con las siguientes calificaciones:

Tipo	Docente	Calificación
Presidente Tribunal De Defensa	Dr. RICAURTE FERNANDEZ, MARVIN JOSE , Ph.D.	10,0
Miembro Tribunal De Defensa	Dr. TAFUR GUISAO, JUAN PABLO , Ph.D.	10,0
Tutor	Dr. CAETANO SOUSA MANUEL , Ph.D.	10,0

Lo que da un promedio de: **10 (Diez punto Cero)**, sobre 10 (diez), equivalente a: **APROBADO**

Para constancia de lo actuado, firman los miembros del Tribunal Calificador, el/la estudiante y el/la secretario ad-hoc.

*Certifico que en cumplimiento del Decreto Ejecutivo 1017 de 16 de marzo de 2020, la defensa de trabajo de titulación (o examen de grado modalidad teórico práctica) se realizó vía virtual, por lo que las firmas de los miembros del Tribunal de Defensa de Grado, constan en forma digital.*



**FIERRO PITA, OSCAR ALEXANDER**  
**Estudiante**

MARVIN JOSE  
RICAURTE  
FERNANDEZ  
Dr. RICAURTE FERNANDEZ, MARVIN JOSE , Ph.D.  
**Presidente Tribunal de Defensa**

Firmado digitalmente por  
MARVIN JOSE RICAURTE  
FERNANDEZ  
Fecha: 2021.07.08 09:37:21  
CS/2021

MANUEL  
CAETANO SOUSA  Digitally signed by  
MANUEL CAETANO SOUSA  
Date: 2021.07.07 19:00:25  
-05'00'

Dr. CAETANO SOUSA MANUEL , Ph.D.  
**Tutor**

JUAN PABLO  
TAFUR GUISAO  Firmado digitalmente por JUAN  
PABLO TAFUR GUISAO  
Fecha: 2021.07.07 17:30:01 -05'00'

Dr. TAFUR GUISAO, JUAN PABLO , Ph.D.  
**Miembro No Tutor**

CARLA SOFIA  
YASELGA NARANJO  Digitally signed by CARLA SOFIA  
YASELGA NARANJO  
Date: 2021.07.07 17:24:58 -05'00'

YASELGA NARANJO, CARLA  
**Secretario Ad-hoc**

**AUTORIA**

Yo, **Oscar Alexander Fierro Pita**, con cédula de identidad 1004296008, declaro que las ideas, juicios, valoraciones, interpretaciones, consultas bibliográficas, definiciones y conceptualizaciones expuestas en el presente trabajo; así cómo, los procedimientos y herramientas utilizadas en la investigación, son de absoluta responsabilidad de el/la autora (a) del trabajo de integración curricular. Así mismo, me acojo a los reglamentos internos de la Universidad de Investigación de Tecnología Experimental Yachay.

Urcuquí, Julio 2021



---

Oscar Alexander Fierro Pita

CI: 1004296008

**AUTORIZACION DE PUBLICACION**

Yo, **Oscar Alexander Fierro Pita**, con cédula de identidad 1004296008, cedo a la Universidad de Investigación de Tecnología Experimental Yachay, los derechos de publicación de la presente obra, sin que deba haber un reconocimiento económico por este concepto. Declaro además que el texto del presente trabajo de titulación no podrá ser cedido a ninguna empresa editorial para su publicación u otros fines, sin contar previamente con la autorización escrita de la Universidad.

Asimismo, autorizo a la Universidad que realice la digitalización y publicación de este trabajo de integración curricular en el repositorio virtual, de conformidad a lo dispuesto en el Art. 144 de la Ley Orgánica de Educación Superior.

Urququí, Julio 2021



---

Oscar Alexander Fierro Pita

CI: 1004296008

## **DEDICATION**

*To my Father and Mother, Fabian and Alicia, to my wife  
Katherine, to my little son Samuel, to my sisters, to my brother,  
and my whole family.*

*Oscar Alexander Fierro Pita*

## ACKNOWLEDGEMENTS

First of all, I would like to thank Yachay Tech University for giving me the opportunity to do my undergraduate studies with the best educational and human quality I could have found. I would also like to thank all the teachers of the institution, especially those who make up the School of Chemical Sciences and Engineering for having dedicated their time, patience, effort and dedication to provide me with their valuable knowledge. I would especially like to thank the GIAMP research group for the honor of being part of it and for trusting me for the development of my titulation project.

Special thanks to my thesis tutors, Professor Manuel and Professor Alex, for helping me at all times in the development of the project and for giving me the necessary confidence to carry it out, overcoming and solving all the challenges that arose at the time.

Thanks to my parents, Fabian and Alicia for always giving me their support and dedicating their lives to my well-being and integral development, to my wife Katherine for giving me her understanding and unconditional support, to my little son Samuel who has become the engine of my life, to my sisters Gaby, Betty and Jessica for their advice and example, to my brother Jairo for teaching me to trust myself, to my niece Milena for always trusting me, to my in-laws, brothers-in-law and all my family and friends.

*Oscar Alexander Fierro Pita*



## RESUMEN

El diseño y construcción de equipos que permitan probar materiales con posibles propiedades fotocatalíticas es de gran importancia en el área de investigación de materiales. En el marco del diseño es necesario tomar en cuenta tres factores principales. El primero de ellos es quizá el más importante y se trata de la fuente de iluminación. El segundo factor que debe ser tomado en cuenta es el fotocatalizador y el tercer factor a tomar en cuenta es el tipo de reactor que se diseñará. En este contexto, el presente trabajo describe el diseño y modelado de un sistema optimizado para pruebas de fotocatalizadores basado en el uso de diodo emisores de luz (LEDs) con una longitud de onda de 365 nm y una potencia de 3.6 W. Se eligieron LEDs como fuente de iluminación, debido a que poseen características favorables como: eficiencia energética, gran expectativa de vida, flexibilidad de diseño, bajo costo, variedad de intensidades y longitudes de onda apropiadas. La simulación de la fuente de iluminación fue realizada mediante herramientas de ingeniería óptica presentes en OpticStudio, un software óptico de la compañía ZEMAX que permitió determinar principalmente la irradiancia óptima de la fuente ( $0.412 \text{ W/cm}^2$ ) y la distancia a la que se deben ubicar los LEDs uno respecto a otro. Seguidamente, se selecciona a la anatasa como modelo de fotocatalizador debido a que este semiconductor en particular es uno de los materiales más usado en reacciones fotocatalíticas debido a la energía de band gap relativamente baja que posee (3.2 eV). Se seleccionó el modo de funcionamiento batch, debido a que se obtienen beneficios como el manejo de volúmenes pequeños de muestras, disminución del tiempo de residencia, fácil control del grado de conversión de la reacción y menor costo asociado a las dimensiones del equipo. Una vez que se obtuvieron los datos referentes a la fuente de iluminación, fotocatalizador y tipo de reactor, se implementa el software Proteus 8 para diseñar el circuito eléctrico obteniendo valores de amperaje (2.69 A) y voltaje (6.07 V). Seguidamente se utiliza el software Autodesk Fusion 360 para diseñar la estructura final de todo el equipo obteniendo las siguientes dimensiones 320 x 193.2 x 180 mm.

**Palabras clave:** Diseño virtual, Pruebas Fotocatalíticas, Irradiación de LEDs, OpticStudio, Proteus 8, Autodesk.

### ABSTRACT

The design and commissioning of equipment for testing materials with possible photocatalytic properties is of great importance in the area of materials research. Three main factors must be taken into account in the design of this system. The first of these is perhaps the most important and concerns the illumination source. The second factor to be taken into account is the photocatalyst and the third factor to be taken into account is the type of reactor to be designed. In this context, the present work describes the design and modeling of an optimized photocatalyst test system based on the use of light emitting diode (LEDs) with a wavelength of 365 nm and a power of 3.6 W. LEDs were chosen as the illumination source because they have favorable characteristics such as: energy efficiency, long life expectancy, design flexibility, low cost, variety of intensities and appropriate wavelengths. Illumination was simulated employing optical engineering tools from OpticStudio, a software from the company ZEMAX, which made it possible to determine the optimum irradiance of the source ( $0.412 \text{ W/cm}^2$ ) and the distance at which the LEDs should be placed with respect to each other. Anatase was selected as a model photocatalyst because this particular semiconductor is one of the most used material in photocatalytic reactions due to its relatively low band gap energy (3.2 eV). A batch mode running was selected due to the advantages that it presents, such as handling small volumes of samples, reducing residence time, easy control of the degree of conversion of the reaction and lower cost associated with the dimensions of the equipment. Once the data regarding the light source, photocatalyst and reactor type were obtained, the Proteus 8 software was implemented to design the electrical circuit, obtaining values of amperage (2.69 A) and voltage (6.07 V). Finally, Autodesk Fusion 360 software was used to modeling the whole equipment's final structure along with the dimensions of 320 x 193.2 x 180 mm.

**Keywords:** Virtual Design, Photocatalytic testing, LEDs irradiation, OpticStudio, Proteus 8, Autodesk.

## CONTENTS

---

### RESUMEN

### ABSTRACT

<b>CHAPTER 1: INTRODUCTION - JUSTIFICATION</b> .....	<b>1</b>
1.1 Introduction .....	1
1.2 Problem statement .....	3
1.3 Objectives .....	3
1.2.1. General objective .....	3
1.2.2. Specific objectives .....	3
<b>CHAPTER 2: THEORETICAL BACKGROUND</b> .....	<b>4</b>
2.1. Heterogeneous photocatalysis .....	4
2.1.1. Advantages and disadvantages of heterogeneous photocatalysis .....	5
2.2. UV Photoreactor Principles .....	6
2.2.1 Light Source .....	7
2.2.1.1. Radiation transfer equation .....	9
2.2.2 Photocatalyst .....	12
2.2.2.1. Titanium oxide (TiO <sub>2</sub> ) .....	12
2.2.3 Reactor Type .....	12
2.3. Modeling and design software .....	13
2.3.1. Principles of OpticStudio by ZEMAX .....	13
2.3.2. Principles of Proteus 8 .....	13
2.3.3. Principles of Autodesk Fusion 360 .....	14
<b>CHAPTER 3: METHODOLOGY</b> .....	<b>15</b>
3.1 Design Premises .....	15
3.2 Design and modeling .....	17
3.2.1. LEDs modeling: OpticStudio by ZEMAX .....	17

---

3.2.2. Electrical circuit design: Proteus 8 .....	23
3.2.3. General structure design: Autodesk Fusion 360 .....	25
<b>CHAPTER 4: RESULTS AND DISCUSSION .....</b>	<b>28</b>
4.1 Light source .....	28
4.1.1. Light source simulation .....	29
4.1.2. LED's distance .....	31
4.1.3. LED's distribution .....	32
4.2 Electrical circuit .....	39
4.3 Reactor structure.....	42
4.4 Equipment sizing.....	45
4.5 Economic estimate (Class V).....	46
<b>CONCLUSIONS AND RECOMMENDATIONS.....</b>	<b>47</b>
<b>BIBLIOGRAPHY .....</b>	<b>49</b>
<b>ANNEX .....</b>	<b>56</b>

## CHAPTER 1: INTRODUCTION – JUSTIFICATION

### 1.1 Introduction

One of the first studies in photocatalysis was reported in 1972 by the pioneers in this area, Fujishima and Honda<sup>1</sup>. In their study, the researchers performed a photocatalytic separation of water molecules, converting them into H<sub>2</sub> and O<sub>2</sub>. From this experimentation, a large number of studies have been developed in the area of heterogeneous photocatalysis, with the main emphasis on the removal of organic pollutants present in water or air.<sup>2,3</sup>

Photocatalysis is defined from different points of view depending on the researcher describing it. However, for the present work, we will take into consideration the definition provided by Braslavsky's research group, which in its work called "Glossary of terms used in photocatalysis and radiation catalysis (IUPAC recommendations 2011)" defines heterogeneous photocatalysis as: "*Change in the rate of a chemical reaction or its initiation under the action of ultraviolet, visible, or infrared radiation in the presence of a substance—the photocatalyst—that absorbs light and is involved in the chemical transformation of the reaction partners.*"<sup>4</sup> Therefore, the reaction can be carried out by artificial light sources or even by sunlight,<sup>5</sup> In this context, it is noteworthy that the use of sunlight as a source of illumination has positive effects on the environment.

Heterogeneous photocatalysis is carried out by oxidation and reduction reactions. That is to say, and the process involves a transfer of electrons from one species that is reduced or gains electrons to another that is oxidized or loses electrons.<sup>6</sup> The electron transfer that takes place between these compounds transforms them into molecular fragments, which are called radicals and are usually volatile and reactive species.<sup>7</sup> The radicals formed are then capable of reacting with other organic or inorganic species, resulting in the formation of thermodynamically stable products, which in most cases are less harmful than the reactive species.<sup>8</sup>

From an experimental point of view, heterogeneous photocatalysis is carried out by using a semiconductor material which is usually an oxide. This material is

---

irradiated with UV or visible light at controlled pressure and temperature conditions. The light emitted in the form of photons comes into contact with the surface of the semiconductor, with the energy required to release an electron, generating a positively charged hole.<sup>9</sup> Subsequently, the species present in the environment are adsorbed in the aforementioned holes, and oxidation and reduction reactions take place, transforming the species into products. This process is widely used for the elimination of microorganisms, inorganic compounds, and pollutants.<sup>10, 11</sup>

Heterogeneous photocatalysis has exceptional applications for the development of green chemistry. However, semiconductor materials with photocatalytic properties have a significant role in the reaction, and therefore their study is of high interest for researchers and scientists.<sup>12</sup> In recent years, a considerable number of materials with possible photocatalytic properties have been synthesized, but before being considered as photocatalysts, they need to be characterized. In this context, investigators are in constant discussion about the best techniques and methods to determine characteristics such as luminous intensity, activation energy or bandgap, electron transfer, and the kinetics of the reactions associated with each material.<sup>13</sup> Photocatalytic reactors are generally used to answer these questions, but in many research laboratories, these reactors are pretty rudimentary, in which case the environmental conditions are difficult to control, and therefore the results cannot be quantified with great accuracy.<sup>14</sup>

The challenge of designing a photocatalytic reactor for the characterization of materials with possible photocatalytic properties is faced within the framework of economic feasibility and operational difficulty. In this context, a previous study of the system is required to analyze essential aspects such as: what could be the most suitable design methodology?, which are the available optimization criteria?, how would be the system performance with a given light source?, and what is known about the reaction kinetics?.<sup>15</sup> Then, it is convenient to develop a preview of the system using simulation tools and physical and mathematical fundamentals.

---

## **1.2 Problem statement**

The development of a system to test materials with possible photocatalytic properties is of great importance for materials research. Generally, the characterization of materials is carried out with equipment assembled in an improvised way with the materials available in a laboratory, such as UV lamps that are usually used in thin-layer chromatography. This practice generates errors associated with the equipment and, therefore, the difficulty in replicating the experiments required to validate a characterization process under controlled conditions.

## **1.3 Objectives**

### **1.3.1 General Objective**

- Design and model of a light emitting diodes-based system for the characterization of materials with potential photocatalytic activity under optimal and controlled conditions and homogeneous irradiation.

### **1.3.2 Specific objectives**

- Select commercial LEDs for the radiation environment that can meet the energy requirements necessary to activate materials with photocatalytic properties.
- Design the LEDs array distribution and simulate the illumination system.
- Design the electric circuit to obtain the values associated with the electrical requirement of the system.
- Design and model a 3D prototype, with the implementation of a computer software, that allows dimensioning the equipment and provides a realistic view of all the components that make up the system and their spatial location

## CHAPTER 2: THEORETICAL BACKGROUND

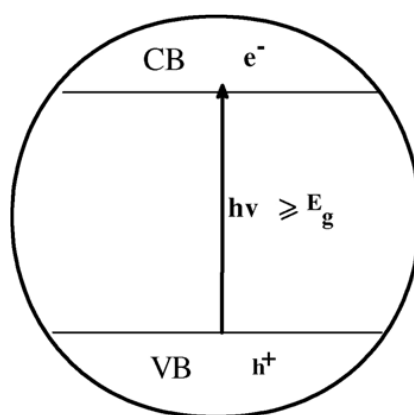
### 2.1 Heterogeneous photocatalysis

Heterogeneous photocatalysis is defined by Braslavsky as: "*Photocatalysis taking place at the interfacial boundary between two phases (solid/liquid, solid/gas and liquid/gas).*"<sup>4</sup> One of the first times that the concept of heterogeneous photocatalysis was reported to the scientific world was in 1921, Baly et al published a scientific article in which they synthesized formaldehyde and carbohydrates from carbon dioxide and water through a photocatalytic process.<sup>16</sup> Since then, research advances in photocatalytic processes have developed rapidly, especially in recent years.

In a heterogeneous photocatalysis process, the activation of the reaction is produced by the interaction between the surface of a photocatalyst and the photons emitted by a light source. To activate the photocatalyst, the energy contained in the photons ( $h\nu$ ) must necessarily be equal to or higher than the bandgap energy of the photocatalyst. It is important to emphasize that the term band gap energy ( $E_g$ ) will be defined in the words of the researcher Braslavsky as: "*Energy difference between the nonconductive and the conductive state of the material. In semiconductors and insulators, it is the energy difference between the bottom of the conduction band (CB) and the top of the valence band (VB).*"<sup>4</sup> If this condition is satisfied, the photocatalytic reaction can initiate.

The interaction of the photon with the surface of the photocatalyst generates the denominated photonic excitation; with this process, a positive hole is generated in the valence layer of the catalyst, and subsequently, the denominated hole ( $h^+$ )-electron ( $e^-$ ) pair is created (see Figure 1).<sup>6, 17</sup>





**Figure 1.** Schematic mechanism of electron-hole pair formation<sup>17</sup>.

Once the electron-hole pair has formed, the species present in the environment are adsorbed on the catalyst surface, triggering a series of oxidation (electron-donating) and reduction (electron receiving) reactions.<sup>6</sup> This process ends when thermodynamically stable products have been formed, which are generally less harmful than the reactive species.<sup>8</sup>

### 2.1.1 Advantages and disadvantages of heterogeneous photocatalysis

Heterogeneous photocatalysis, as an industrial-scale or laboratory-scale process, can be used for a wide variety of purposes, including the degradation of organic and inorganic compounds, hydrogen production, air purification, elimination of bacteria or pathogenic microorganisms, and even the elimination of SARS-COV-2.<sup>18,19,20</sup> Compared to other conventional methods with similar applications, photocatalysis has shown more significant growth and development among researchers, who have paid great attention to it due to the advantages that this process offers, especially in terms of economy and efficiency.<sup>7, 18</sup>

One of the most notable advantages of heterogeneous photocatalysis is its eco-friendly nature. It is a method that reduces the pollution associated with the removal of specific pollutants by conventional techniques such as chlorination.<sup>21</sup> This argument is supported by the fact that a photocatalysis reaction can be carried out even if the light source is the sun, thus eliminating the cost of electricity and material associated with an artificial source.<sup>22, 23</sup> On the other hand, photocatalytic

reactions require only the photocatalyst for their correct development, thus reducing the need to implement a large amount of polluting chemical compounds.<sup>24</sup>

Photocatalytic reactions have different kinetics, depending on the reagents. However, the materials needed to set up a controlled photocatalysis system are generally the same.<sup>25</sup> In this sense, a photocatalysis process can be carried out under atmospheric pressure and ambient temperature conditions.<sup>10</sup> Therefore, no additional equipment is required to control these variables, thus reducing the cost associated with the process and the system. Moreover, there is no need to add oxygen to the system in pollutant removal or degradation reactions since the oxygen present in the environment is sufficient to generate radicals.<sup>26</sup>

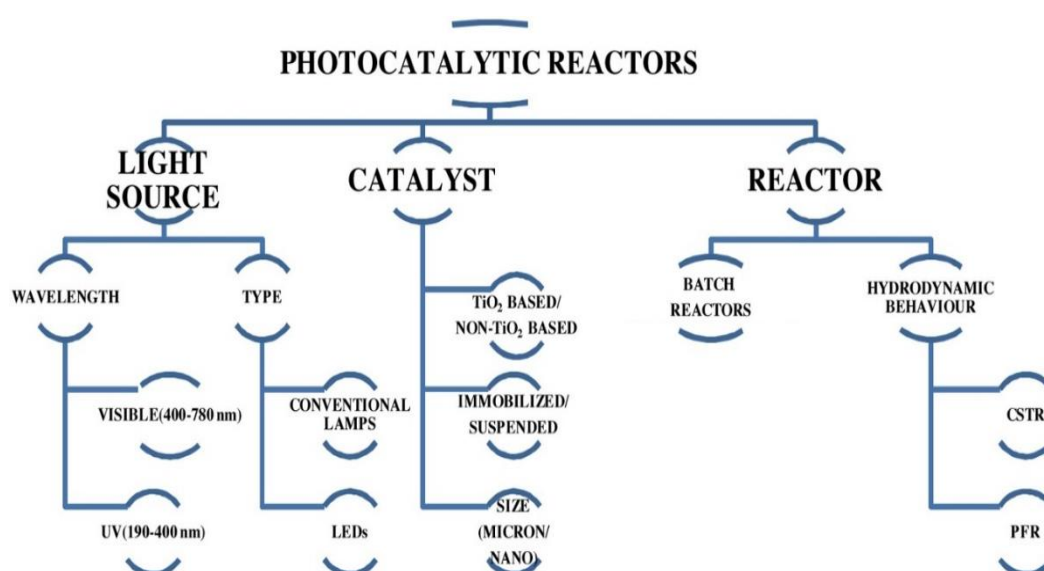
Heterogeneous photocatalysis has several advantages; however, the disadvantages associated with this process cannot be ignored. One of the most notable drawbacks is related to the light source, since the more significant the magnitude of the wavelength, the more difficult and time-consuming the catalyst activation process will be.<sup>23, 27</sup> It is significant to emphasize that there are some microorganisms resistant to specific wavelengths and therefore represent greater design challenges.<sup>2, 28</sup> Finally, a disadvantage that cannot be overlooked is the fact that, in some reported experiments, the photocatalyst is used in the form of nanoparticles. In this sense, the recovery of the photocatalyst, at the end of the reaction can only be carried out using special cellulose-based filters, which considerably increases the cost of the process and the difficulty of its scaling up.<sup>29</sup>

## **2.2 UV Photoreactor Principles**

The study of heterogeneous photocatalysis is having a far-reaching impact on many fields of research, especially in recent years. In this context, the main areas, in terms of academic interest, have been mainly organic chemistry, physical chemistry, chemical kinetics, and materials science.<sup>14</sup> However, research in the area of chemical engineering and reactor development for photocatalysis has not been considerably high. Therefore, very few industrial processes in this field have been developed.<sup>30</sup>

---

According to Braslavsky<sup>4</sup>, a photocatalytic reactor can be defined as a type of reactor used to determine the yields of photo-adsorption and photocatalytic reactions with a catalyst in the form of a sprayed layer or a solid-state film. The incident photons are absorbed by the catalyst, provided that the scattering layer is sufficiently thick (or the scattering is enough concentrated). In this sense, it is possible to classify photocatalytic reactors based on three main factors: light source, photocatalyst, and reactor type, as can be seen in Figure 2.<sup>14</sup>



**Figure 2.** Classification of Photocatalytic Reactors.

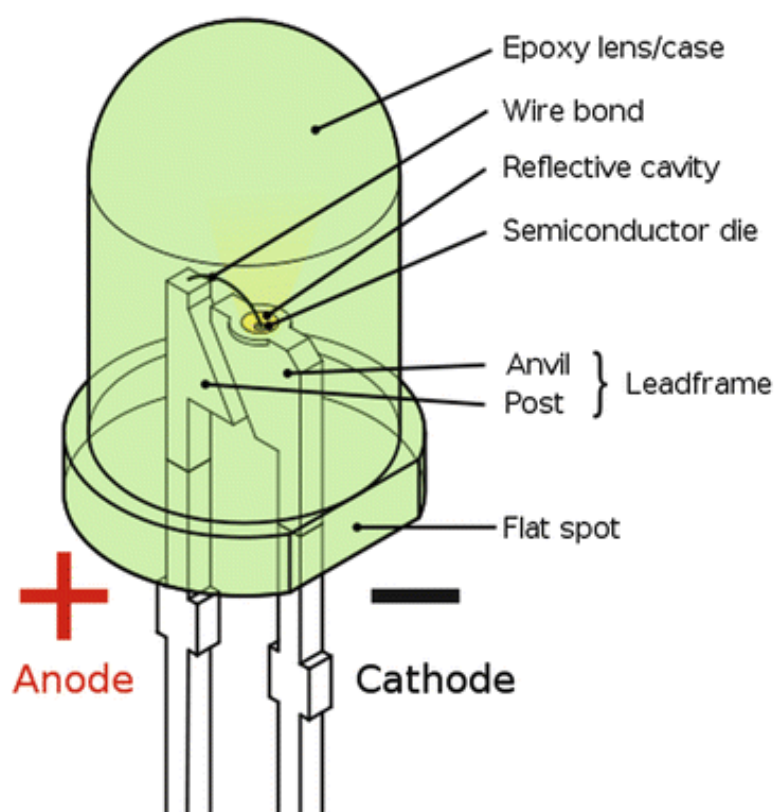
The development of the proposed photocatalytic reactor model requires a previous understanding of the main parameters of the system. Among the most important are the characteristics of the radiation source and the reaction kinetics suggested by the reactants. Additionally, it is necessary to know how these characteristics are related to making the equipment.<sup>14</sup>

### 2.2.1. Light Source

The source selection criteria are of vital importance in the process since UV radiation is the heart of the whole process. The radiation sources that make up a photocatalytic reactor can be sunlight, conventional UV lamps, and light-emitting

diodes (LEDs).<sup>31</sup> In this sense, sunlight is not a suitable source for a laboratory-scale model since it depends on several climatic factors. Conventional lamps are also not appropriate sources for the system since they have low efficiency in terms of the electrical power they require in relation to the light energy they emit. Additionally, the physical structure of conventional lamps makes the design criteria for the reactor considerably more difficult.<sup>32</sup>

LEDs have superior efficiency compared to their competitors. Additionally, LEDs are less expensive than conventional lamps and have a longer life expectancy without the need for toxic components (see figure 3).<sup>33</sup>



**Figure 3.** The internal architecture of a UV LED light bulb.

LEDs undoubtedly denote remarkable features, and their development in recent years has advanced systematically to reach higher standards. Thus, designing a system whose light source is LEDs can offer much more than just a more powerful source, as these devices provide countless design opportunities and can even be implemented to improve existing equipment.

### 2.2.1.1. Radiation Transfer Equation

The distribution of the emitted energy can be considered as the parameter that governs the kinetics of the photoreactions. The mathematical model that can describe the radiant energy field of a point source is obtained from the radiation transfer equation (RTE), which represents the propagation of radiation in a 3D medium with absorption, emission, and scattering.<sup>34</sup> For this, it is necessary to apply the finite volume method, in which it is assumed that the density and mass in a given volume remain constant. This is possible since a photocatalytic reactor is a discrete space, and the photons emitted by the radiation source have direction based on solid angles.<sup>35, 36</sup> Once the RTE is solved under the above assumptions, the so-called photon balance equation is obtained, which can be solved for basic geometries, including small cylinder volumes, and allows obtaining the radiative heat transfer.

Radiative heat transfer is obtained for each unit vector, which denotes the position of the photons and therefore has a fixed wavelength. Mathematically, the radiation transfer equation can be obtained by the following energy balance:<sup>37</sup>

$$\begin{aligned} &(\text{outgoing intensity} - \text{incoming intensity}) + \text{absorbed intensity} + \text{outgoing} \\ &\text{scattered} = (\text{incoming emission} - \text{outgoing emission to other parts}) + \text{incoming} \\ &\text{scattered} \end{aligned}$$

$$\begin{aligned} \nabla [\Omega I_\lambda(s, \Omega, t)] + k_\lambda(s, \Omega, t) I_\lambda(s, \Omega, t) + \sigma_\lambda(s, \Omega, t) I_\lambda(s, \Omega, t) = \\ j_\lambda(s, t) \int_{\Omega'=4\pi} \Psi(\Omega' \Omega) I_\lambda(s, \Omega', t) d \Omega' \end{aligned} \quad (1)$$

where:

$s$ : The position vector

$\Omega$ : Directional unit vector

$t$ : Time

$I_\lambda(s, \Omega, t)$ : Radiant intensity for a specific solid angle, location, and time

$k_\lambda$ : Absorption coefficient of the medium

$\sigma_\lambda$ : Scattering coefficient of the particulates in the medium

$j_\lambda$ : Radiation emission

$\Psi(\Omega' \Omega)$ : Phase function

For a system operating at low temperatures (room temperature), the emission can be neglected. Additionally, if we consider that there are no particles or bubble formation in the system, Eq (1) can be simplified as follows:

$$\frac{dI(s, \Omega)}{ds} + k(s, \Omega)I(s, \Omega) = 0 \quad (2)$$

$$I(L, \Omega) = I_0(\Omega) \exp\left(-\int_0^L k(s, \Omega) ds\right) \quad (3)$$

Where:

$I(L, \Omega)$ : Radiant intensity at a distance L with a specific solid angle  $\Omega$

$I_0$ : Radiant intensity at the source

$k$ : Local absorption coefficient

$L$ : Distance from the source to the receptor

$\Omega$ : Specific solid angle

Equations (2) and (3) are commonly known as the Beer-Lambert equation for stationary conditions and are in both differential and integral forms.<sup>38</sup> Applying the definition of radiant intensity in the above equations yields the received fluence rate ( $G$ ) whose units are ( $W/cm^2$ ):

$$G(L, \Omega) = \frac{1}{L^2} I_0(\Omega) \exp\left[-\int_0^L k(s, \Omega) ds\right] \quad (4)$$

In this way, the main equation of the mathematical modeling process Eq. (4) is obtained, which allows the development of a mathematical model for any type of point radiation source.<sup>37</sup>

In the proposed photocatalytic reactor, the light rays emitted by the light source need to pass through certain materials to reach the surface of the photocatalyst. In this context, each medium has its own refractive index Eq. (5), expressed as follows:

$$n = \frac{c}{v_p} \quad (5)$$

Where:

$n$  = Refractive index

$c$  = Speed of light in vacuum

$v_p$  = Phase velocity

The refractive index is understood as a measure of how much the beam velocity is affected when passing through a certain material.<sup>39</sup> This magnitude will help to determine the energy loss from the source to the surface of the catalyst, allowing us to know if the latter will be activated or not.

On the other hand, the refraction angle of the light beam can also be altered. This could happen when crossing the separation surface between two propagation media, as long as these have a different refractive index. This phenomenon can be described mathematically using the so-called Snell's law Eq. (6), which states that the multiplication of the refractive index by the sine of the angle of incidence with respect to the normal, is constant for any beam of light incident on the surface of the media.<sup>40</sup>

$$n_0 \sin (\theta_0) = n \sin (\theta) \quad (6)$$

Where:

$n_0$ : Refractive index of the medium from which the light beam is emitted.

$\theta_0$ : Angle of incidence.

$n$ : Refractive index of the medium in which the light beam is transmitted.

$\theta$ : Angle of refraction.

The above-described equations are used to characterize a ray of light emitted by the light source. However, to design and model a complete source it is necessary to trace up to a million rays, which would mean repeating the calculations associated with the equations described above a million times. Due to the large number of iterations required to model the illumination system of a photocatalytic

---

reactor, the simulation of the light source can be performed by an optical software. In this context, a software called OpticStudio, developed by the company ZEMAX, has been selected. It is important to mention that this company is a world leader in the development of optical simulators for academic and research purposes.

### **2.2.2. Photocatalysts**

The synthesis of photocatalyst materials has increased in the last decade. In general, research in this area focuses on finding the best catalyst for a non-conventional light source such as solar or synthetic but novel light sources such as LEDs.<sup>41</sup> Each photocatalyst has an associated activation bandgap energy; therefore, before selecting a catalyst, it is crucial to know the wavelength associated with the process and the reaction kinetics of the process.<sup>17</sup>

#### **2.2.2.1 Titanium oxide (TiO<sub>2</sub>)**

Titanium oxide is one of the most promising semiconductor materials currently used in photocatalysis. This is because it has a low level of toxicity; additionally, it is a species with high chemical stability and has a high photocatalytic activity due to its relatively low bandgap (3.2 eV).<sup>42, 43</sup> On the other hand, an essential factor to take into account is that titanium oxide presents polymorphism and therefore each species has a different structure and therefore has different characteristics even if it is the same material.<sup>44</sup> Anatase used in photocatalytic reactions is commercialized as nanoparticles in the order of 10 nm or less. In that state, it can be used directly as a photocatalyst in suspension. However, when the reaction is finished, recovering this species is a challenge.<sup>45</sup> For this reason, the photocatalyst should be fixed on active support that can be formed by polymers, zeolites, and some metal oxides.<sup>46, 47, 48</sup> In this way, the recovery of the catalyst at the end of the reaction should be a much simpler process.

### **2.2.3. Reactor Type**

Photocatalytic reactors can be designed in batch, continuous or recirculating batch mode. They can also be modeled according to the hydrodynamic regime as a

---



continuous stirred tank reactor (CSTR) or a plug flow reactor (PFR).<sup>14</sup> In this context, an appropriate selection of the reactor type allows maximizing the efficiency of the material characterization process since the system can work according to the optimal requirements in terms of sample volume and homogeneity. On the other hand, each type of reactor presents positive and negative characteristics that must be balanced to obtain the best selection criteria.<sup>49</sup>

Continuous flow reactors are the most widely used on large scale because they can handle large volumes of liquids associated with high homogeneity and a high degree of conversion.<sup>50</sup> These systems also facilitate automatic production control, since once the system starts up, the reactions proceed automatically and successively until the entire required volume is treated. However, in equipment designed for the characterization of materials at a laboratory scale, this type of reactor is not suitable. This is due to factors such as the high initial cost of the system, the unnecessary energy investment associated with the formation of a flow, the difficulty of applying the equipment for reactions that have high residence times, and the difficulty related to the homogenization of the radiation from the light source.<sup>51</sup>

Batch reactors are characterized by working at a constant volume which, compared to continuous flow reactors, can be considerably smaller.<sup>52</sup> For this reason, batch reactors are used for small-scale or laboratory scale operations to test new processes that have not yet been developed or to characterize certain materials. The main characteristics of this type of reactor are (i) the high degree of conversion in relatively short reaction times, (ii) the ease of cleaning and maintenance of the equipment, (iii) the low cost associated with the initial implementation, and (iv) the high control obtained in terms of homogeneity and operational conditions.<sup>53, 54</sup>

## **2.3. Modeling and design Softwares**

### **2.3.1. Principles of OpticStudio by ZEMAX**

The software stands out mainly for presenting a complete and very intuitive interface, which very few similar design programs have. There are several companies dedicated to the development of simulators for optical systems, and

---

among the most notable is ZEMAX. It is briefly described as a large company in charge of designing and marketing optical design software with licenses accessible to institutions and commercial organizations. Among its various products, the most notable is called Optic Studio (ANNEX 1), which is a general-purpose optical design program that can be implemented on Microsoft Windows. The software is specifically designed to model imaging and illumination systems by tracing rays that travel through an optical system to a reader called a receiver.

### **2.3.2. Principles of Proteus 8**

Proteus 8 software is a complete electronic design system that combines an advanced schematic capture program, a mixed (analog and digital) simulation system based on Spice, and a program for component layout and auto-routing. This software belongs to Labcenter Electronics and is one of the simplest systems to use but with impressive computational power. In this sense, the interactivity offered by Proteus 8 allows to increase the user's interest since almost accurate responses are obtained in response to stimuli such as moving a pointer or actuating a pushbutton.

### **2.3.3. Principles of Autodesk Fusion 360**

Autodesk Fusion 360 is a design and modeling software for a wide variety of products and prototypes. This software stands out from its competitors due to its ability to combine industrial design, mechanical design, CAD interfacing, and locomotion in a single program (ANNEX 2). The tools and environment presented by Fusion 360 allow for a complete exploration of any idea to make it a reality. Additionally, the system is compatible with Mac and Windows, so its range of applications increases considerably.

## CHAPTER 3: METHODOLOGY

### 3.1. Design Premises

The design premises selected for the modeling and simulation of the equipment have been chosen based on the arguments presented in the previous sections and depending on the materials available on the market. The table 1 specifies all the design premises for each component and for the equipment in general.

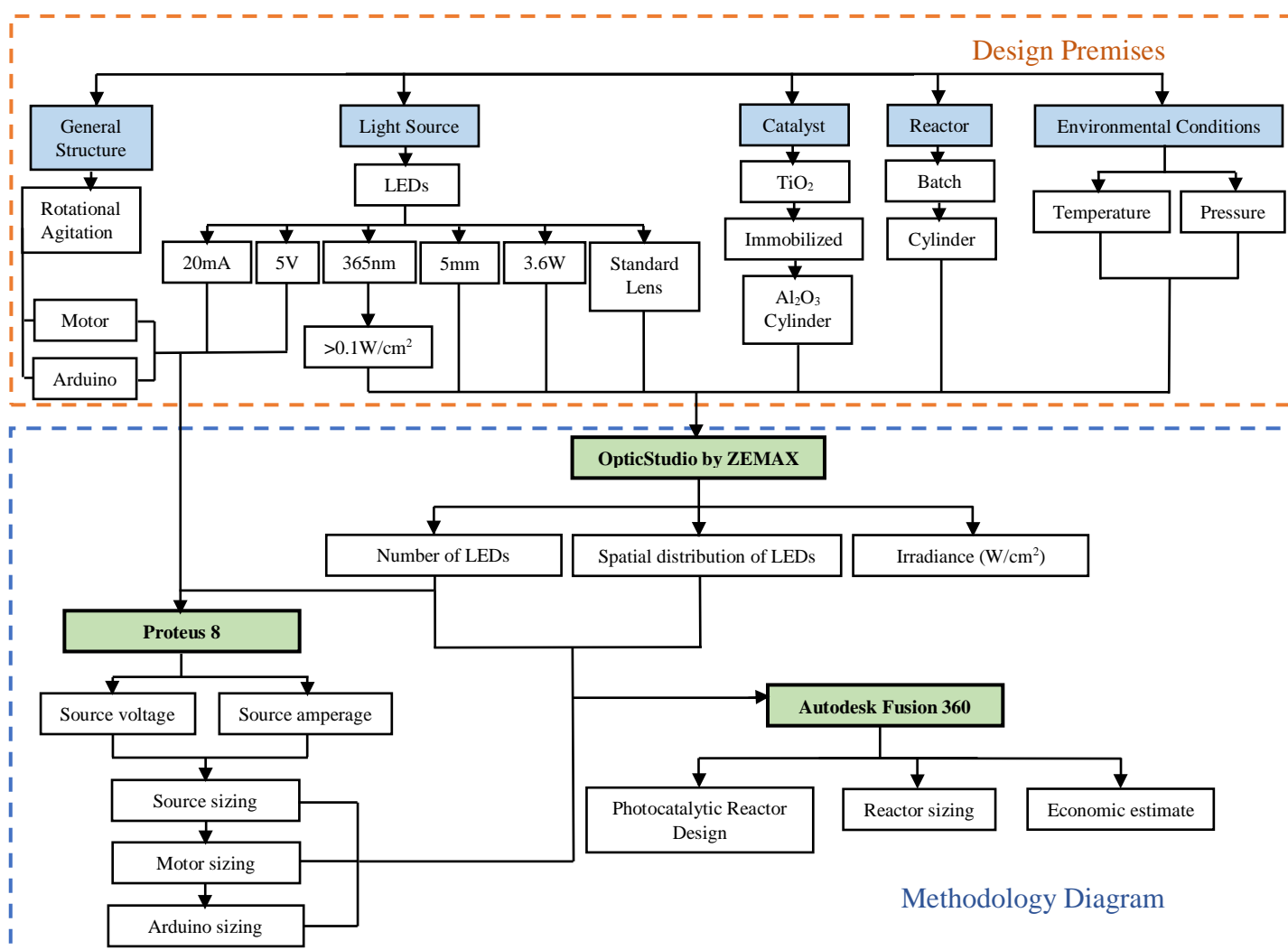
**Table 1.** Design premises.

	<b>Characteristics</b>
<b>Light Source</b>	Light emitting diodes (LEDs)
	Dimensions: standard (5mm)
	Wavelength: 365 nm UV
	Voltage: 5 V
	Power: 3.6 W
	Intensity: 20 A
	Standard Lens
<b>Catalyst</b>	TiO <sub>2</sub>
	Immobilized
	Cylindrical alumina support
	Band gap energy: 3.2 eV
	Irradiance of TiO <sub>2</sub> (W/cm <sup>2</sup> ): 0.0878
	Optimal Irradiance (W/cm <sup>2</sup> ): 0.1
<b>Reactor</b>	Batch
	Cylindrical
	Rotational agitation
	Horizontal orientation
	Detachable
<b>General system</b>	Programmable rotation
	Rectangular structure
	Portable and easy to handle
<b>Environment conditions</b>	Pressure: 1 atm
	Temperature: 20 C

The present system should allow photocatalysis to be carried out under controlled and replicable conditions. In the first instance, the equipment consists of

a reactor, in which one sample can be analyzed for each experiment. However, the expectations of the design are focused on multiplying the number of reactors to increase the number of samples to be analyzed simultaneously and reduce the time involved in characterization with replication of results.

Once the design assumptions have been determined, the modeling of the main components can begin and then the equipment can be designed and sized. This process is carried out in a systematic and orderly manner as shown in Figure 4.



**Figure 4.** Design Premises and Methodology Diagram.

### **3.2. Design and modeling**

For the modeling and simulation of a photocatalytic reactor, the most important factors to take into account are firstly the light source and secondly the type of photocatalyst to be used. Once the parameters have been determined, it is possible to set up a prototype using modeling and system simulation software.

The first one is a software called Autodesk Fusion 360 to model the general structure of the whole system, including the agitation mechanism, lighting, and handling of the equipment. The second software used is from the company ZEMAX and is called OpticStudio, in which the light sources and their interaction with the materials that make up the equipment and the photocatalyst will be modeled. Finally, the third software used is Proteus 8 because this program is used to design electronic circuits as well as the electronic circuit that will be required to provide energy to the system.

Once the modeling and simulation process of the system has been completed in each of the selected software, the equipment can be dimensioned in such a way that it can comply with all the necessary specifications to carry out the photocatalysis reaction. Moreover, the modeling of the system allows having an approach on how the equipment would be once assembled, also allowing to calculate the economic feasibility and, therefore, the impact in the materials research.

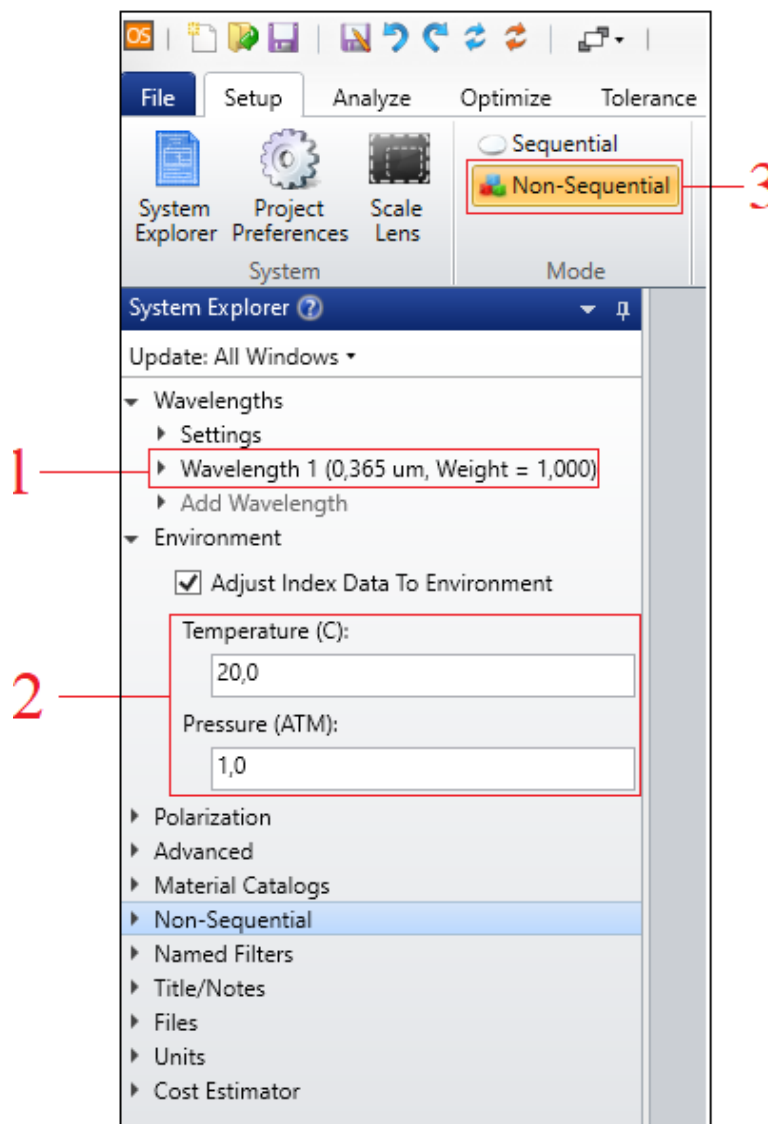
#### **3.2.1. LEDs modeling: OpticStudio by ZEMAX**

This section briefly denotes the design process of a virtual prototype of a LED using OpticStudio to obtain a light transfer model from the source to the desired distribution. For this purpose, the design process is separated into different stages, in which both the physical dimensions and the performance specifications of the LED will be implemented. It is important to emphasize that this design is based on a commercial LED with certain specifications and economic feasibility.

To design an LED, it is first necessary to enter in the software (see Figure 5) data concerning the wavelength (1), the environmental conditions (2), and the ray propagation mode (3). The first two values are determined in terms of exemplification and may vary according to the designer's needs. However, the

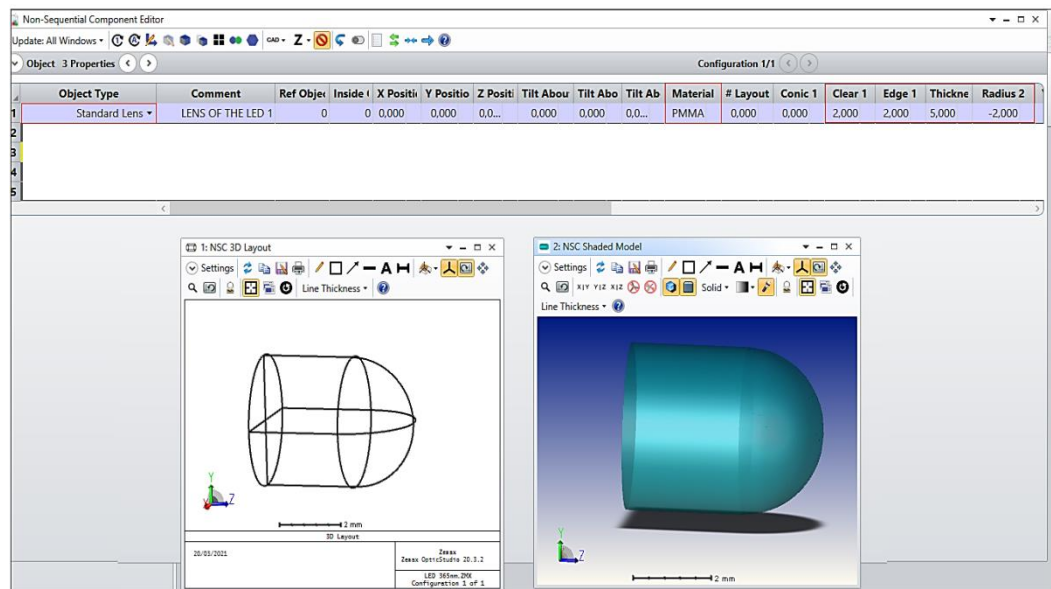
---

lightning propagation model must necessarily be non-sequential. This choice is based on the concept of non-sequential ray propagation, which denotes the following: "Non-sequential ray tracing implies that there is no predefined sequence of surfaces on which the rays to be traced must strike. The objects on which the rays strike are determined solely by the physical positions and properties of the objects, as well as by the directions of the rays." Thus, non-sequential ray-tracing brings the design closer to reality because it does not disregard the shock or deflection of the rays from the source as they interact with the objects in their path.



**Figure 5.** Main parameters in OpticStudio.

The second step is to model the source lens. To do this, the standard lens is selected, and the zero points of the three axes are taken as the spatial location, thus creating the first reference point of the system. Then it is necessary to select the material of which the lens is composed, which in this case is called PMMA. This highly transparent polymer is widely used for the manufacture of lenses because it is scratch-resistant. To finish this step, it is necessary to denote the dimensions of clear, edge, thickness, and radius as shown in Figure 6.



**Figure 6.** Lens design in OpticStudio.

Once the LED lens has been designed, the next step is to implement an internal mirror lens. This element is in charge of directing the rays coming from the source, and its data is entered in the same way as in the previous case, except for the material (MIRROR) and the spatial location (inside of). Regarding this last aspect, it is only necessary to reference and locate the new object from the previously designed lens so that it is automatically and accurately placed (see figure 7).

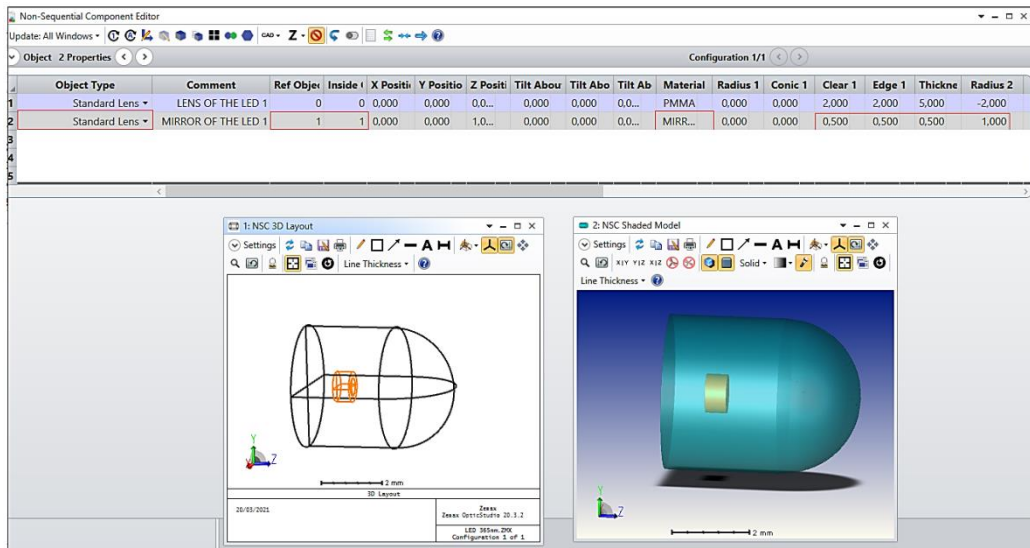


Figure 7. Mirror lens design at OpticStudio.

The next component to be designed is a point source since this element is in charge of emitting the rays. To do this, it is necessary to select the object called Source Volume Rectangle and provide the required data such as the number of analysis rays, the number of observation rays, source power, referenced spatial location, clear and radius, as shown in Figure 8.

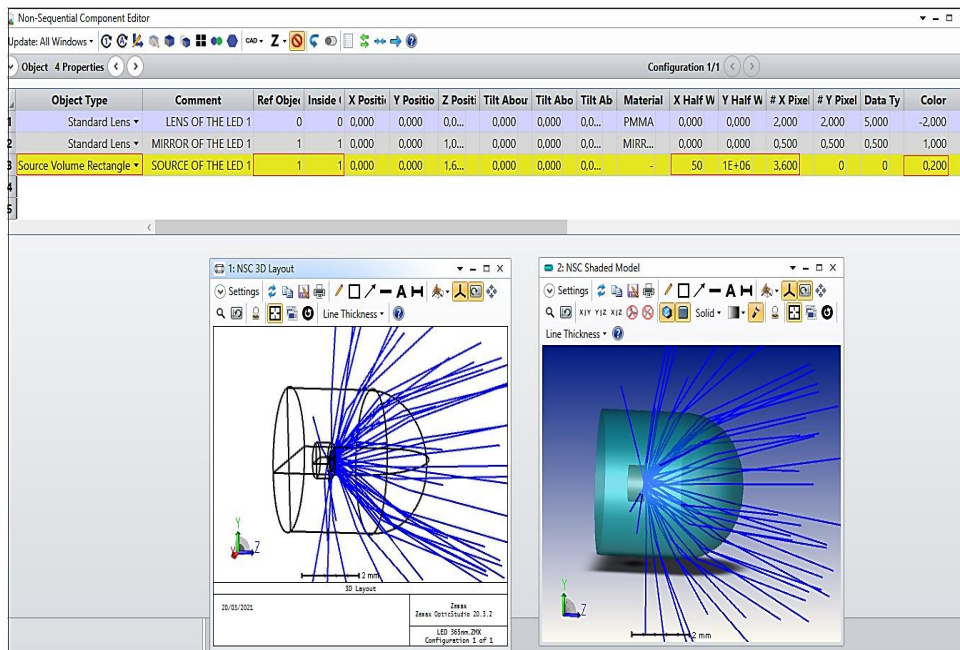
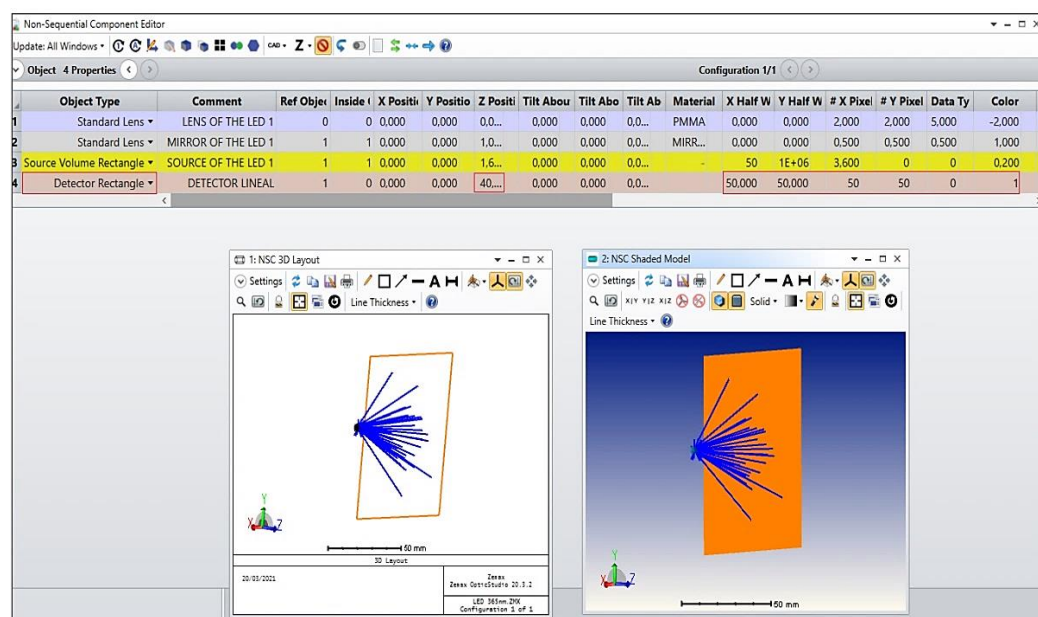


Figure 8. Point source design in OpticStudio.



Next, since the objective of the software is to measure the irradiance emitted from the source with the determined characteristics, it is necessary to implement a component called a detector. This component is in charge of capturing the emitted rays and transforming this information into numerical values in units of  $\text{W}/\text{cm}^2$ . The detector in the software is called a rectangle detector, and its dimensions are placed in the same way as the previous objects. The peculiarity of this component is that the distance from the source is variable, and therefore the irradiance also varies with respect to this parameter. In this case, it is not necessary to determine a specific material. However, the main characteristic of this element is that it has no refractive index and therefore does not intervene in the redirection of the rays, as shown in Figure 9.



**Figure 9.** Receiver design in OpticStudio.

Finally, it is necessary to place the materials that must pass through the beams. For this particular design, it is a pyrex tube and a specific volume of water until reaching the surface of the catalyst. These factors can be designed using the cylinder volume option, which allows entering values concerning material (WATER, PYREX), thickness, length, and of the spatial location, as shown in Figure 10.

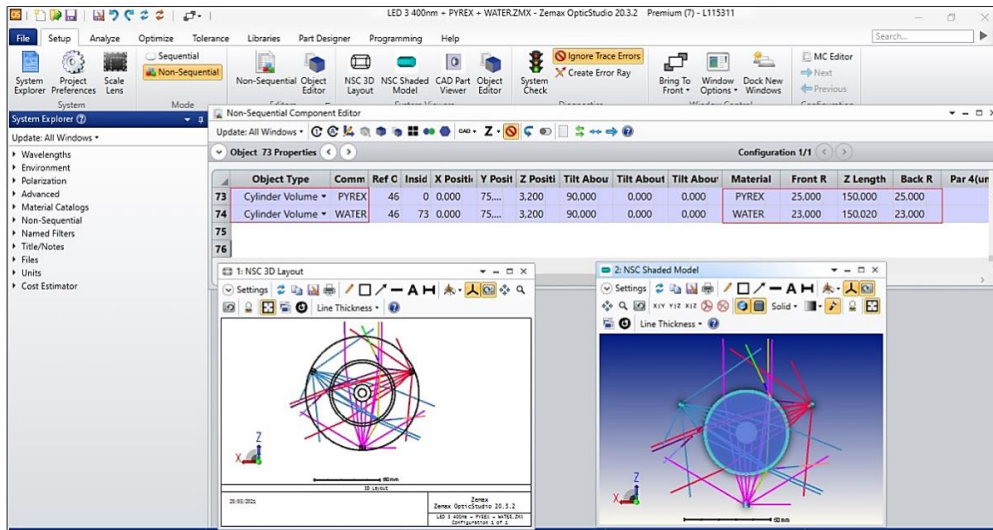


Figure 10. Pyrex cylinder design and water volume at OpticStudio.

Consequently, for the system to work, it is necessary to trace the rays as shown in Figure 11, which allows generating a more realistic graphical representation of the system behavior. Finally, the procedure must be replicated to create a more significant number of LEDs and, if necessary, implement additional materials that the rays must pass through, e.g., the Pyrex cylinder and the volume of water.

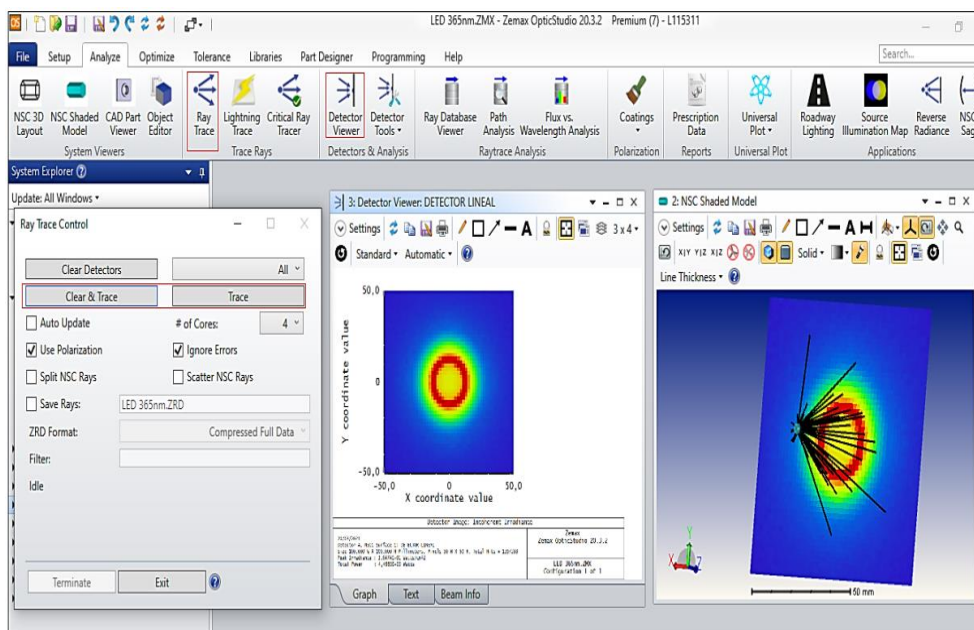
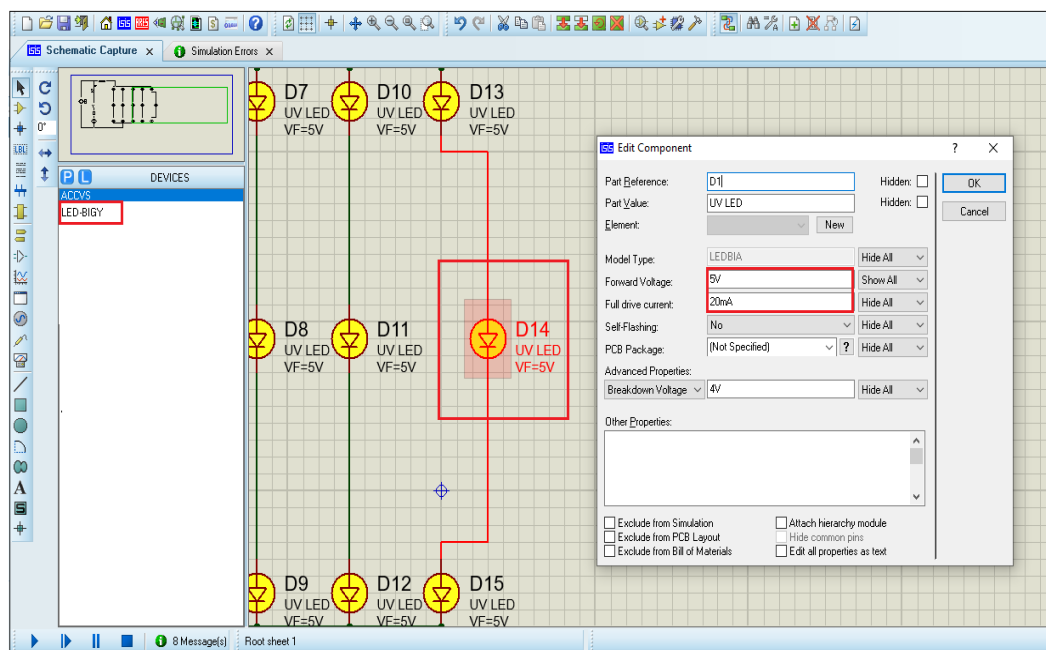


Figure 11. Ray tracing in OpticStudio.

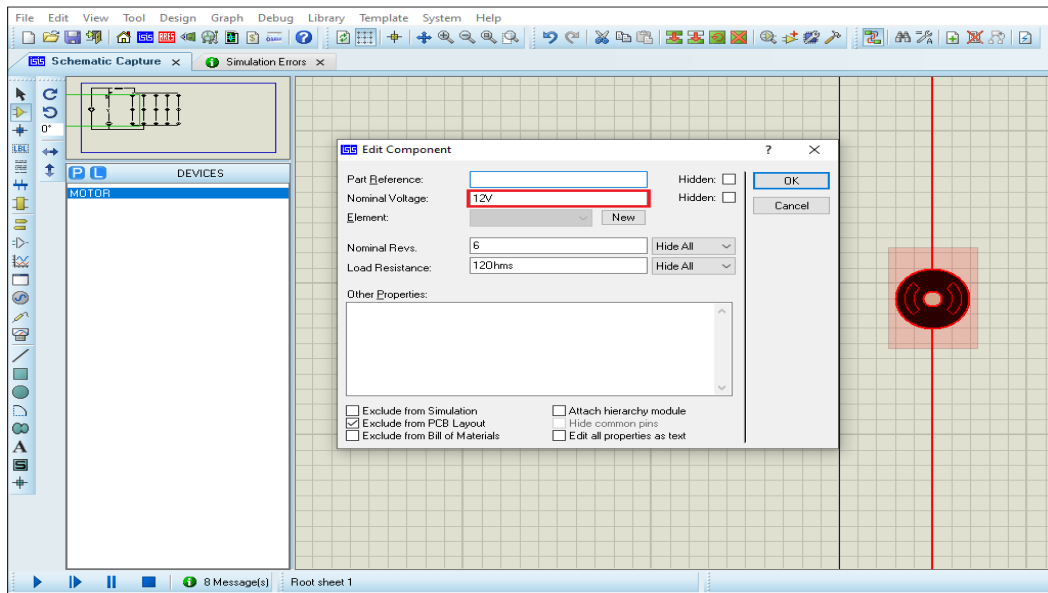
### 3.2.2. Electrical circuit design: Proteus 8

For the current project, it is necessary to simulate the electrical circuit associated with the materials testing system being designed. To do so, we have started with the design of a light emitting diode with defined characteristics. As shown in Figure 12, the first step is to select the LED-BIGY component from the digital catalog. Next, characteristics such as voltage and current intensity needed to turn on the LED must be specified, as well as other sections such as the name and color of the LED.



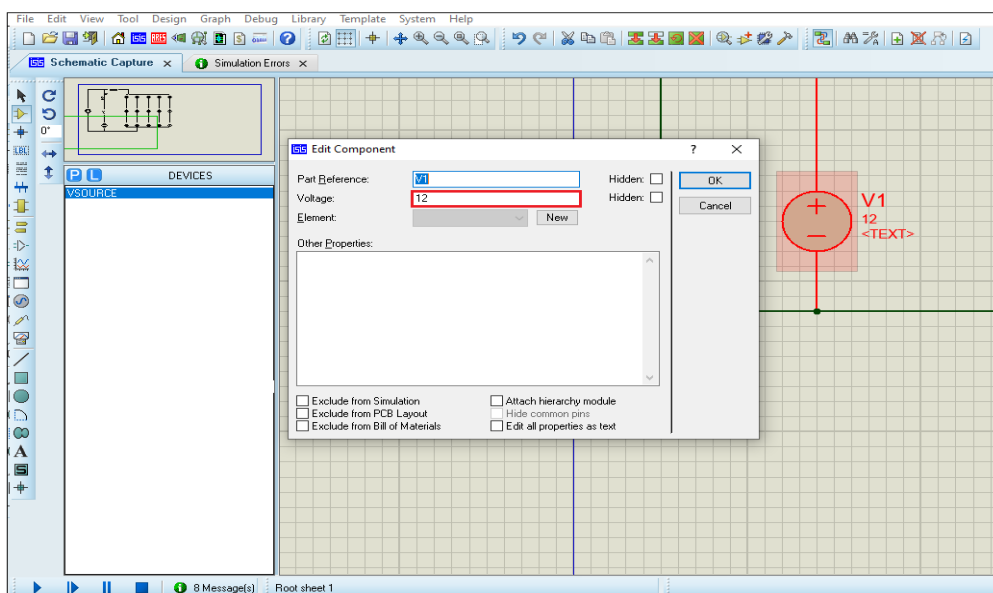
**Figure 12.** Design of an LED in Proteus 8.

Once the light emitting diode has been designed, it is necessary to implement a stepper motor. This type of component is widely used in 3D printer manufacturing and generally operates with voltages lower than 12V. As shown in Figure 13, such a motor can be designed by selecting the component called MOTOR from the catalog, and the voltage data associated with the element is included. It is important to emphasize that the parameters that are filled in should not be altered for this purpose.



**Figure 13.** Design of an engine in Proteus 8.

Next, it is necessary to implement a voltage for the operation of the system. For this purpose, the VSOURCE component is selected from the catalog, and a value of 12V is assigned to it since this voltage is the one generally found in commercial power supplies. All other deals should be left as default, as shown in figure 14.

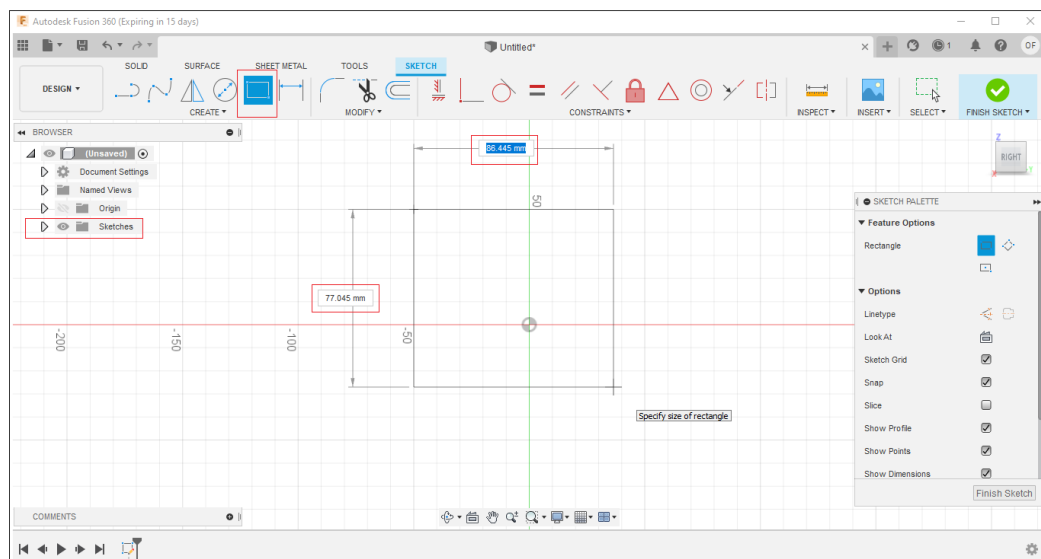


**Figure 14.** Design of a voltage source in Proteus 8.

Finally, the number of LEDs to be implemented must be replicated, and the whole integrated system must be connected. In this way, it is possible to obtain the voltage and current data required by the circuit and accordingly select the commercial components that meet these specifications.

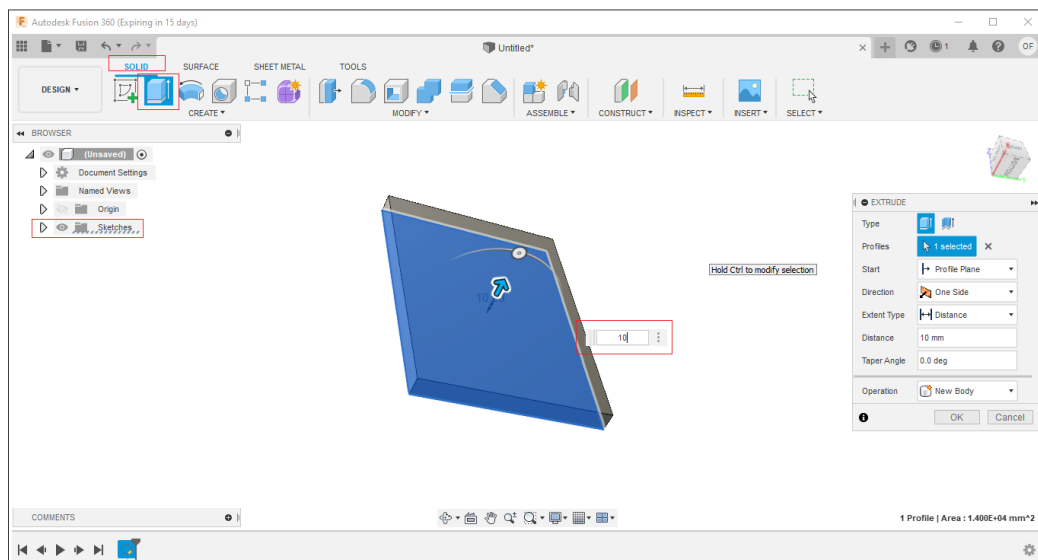
### 3.2.3. Principles of Autodesk Fusion 360

To model the design of a system, it is necessary to know its dimensions and structure. Once this is determined, the first step is to create a template (see Figure 15). This template must include all the exact measurements to generate the design. It is important to emphasize that the software units are specified by default, and since it is a system connected to the Internet, the autosave tool is permanently active.



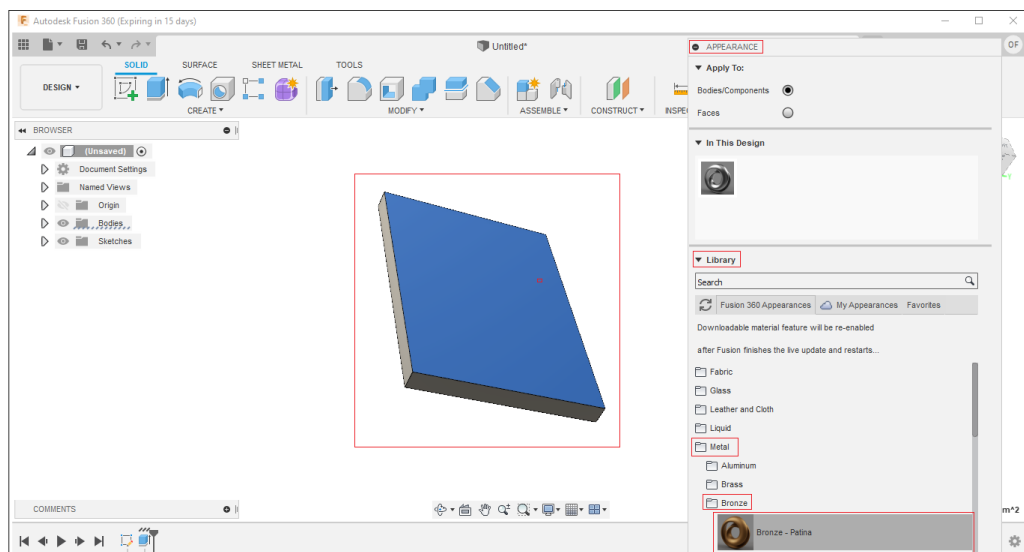
**Figure 15.** Creating a template in Autodesk Fusion 360.

Once the exact dimensions of the template have been determined, it is necessary to convert it into a solid body. To do this, it is needed to select the SOLID option and then enter the thickness. In this way, any desired shape can be obtained, since the templates have all the basic geometric shapes in addition to the accessible design tool (see Figure 16).



**Figure 16.** Creation of a solid in Autodesk Fusion 360.

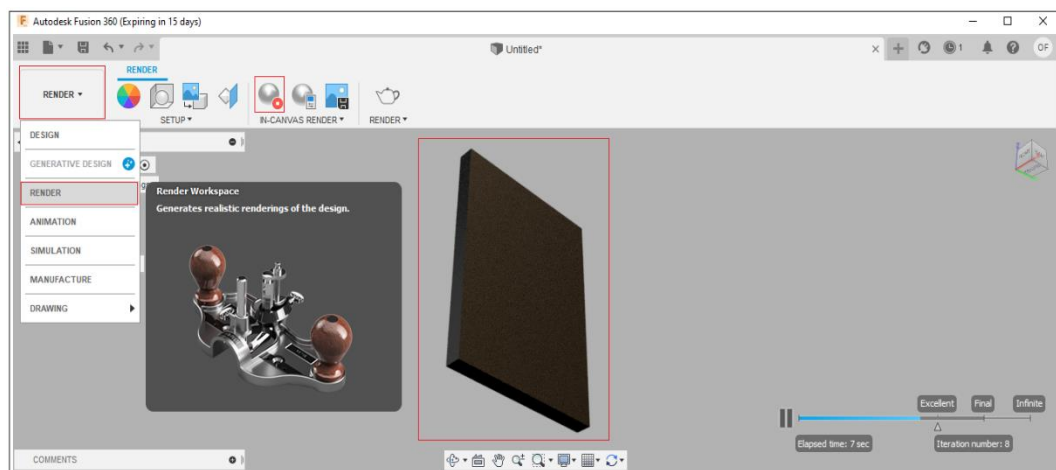
After the solid design is ready, it is necessary to implement the material with which the component is expected to be manufactured. To do this, it is necessary to enter the APPEARANCE option, then a menu of options is displayed in which you can find all types of materials, from metals to polymers. Besides, aspects such as color, brightness, and intensity of shades can also be modified (see Figure 17).



**Figure 17.** Implementation of materials in Autodesk Fusion 360.

The process described above should be followed to design the entire system, however more practice time is required for the more complex parts. In this context, it is important to emphasize that the design must respect the lines and dimensions obtained from the use of the previous software. That is, Autodesk Fusion 360 is the last software to be implemented since it takes as input information those parameters that have been previously determined such as the total number of LEDs and the dimensions of the physical components required by the system.

When all the solid components have been designed and are forming a complete system, it is possible to enhance the design experience with the RENDER option. Thanks to this feature, it is possible to bring the design as close to reality as possible (see Figure 18).



**Figure 18.** RENDER in Autodesk Fusion 360.

The software allows to automatically replicate the desired components, for example to design the complete set of LEDs. Additionally, it is possible to implement motion to certain parts of the equipment to understand the mechanical operation associated with it. This option can be implemented in gear systems, pulleys, agitators, or even in fluids that are in motion.

Finally, it is necessary to propose a final dimensioning of all the equipment, which will allow a general calculation of the cost associated with it. In this context, a cost ratio equivalent to three times the market price of each component, associated to factors such as design time, optimization, manufacturing and possible setbacks, will be taken as a basis for calculation.



## CHAPTER 4: RESULTS AND DISCUSSION

### 4.1 Light source

Light-emitting diodes (LEDs) are semiconductor devices that can emit radiation at a particular wavelength with physical dimensions considerably smaller than other devices with the same function.<sup>56</sup> In this context, the main advantages of LEDs are (i) working at much more powerful wavelengths, (ii) energy savings, (iii) longer life expectancy, (iv) a considerably lower economic investment that does not limit the design of equipment associated with these devices, and (v) the most important is undoubtedly the energy efficiency related to photocatalytic processes.<sup>57</sup>



**Figure 19.** Selection of the LED.

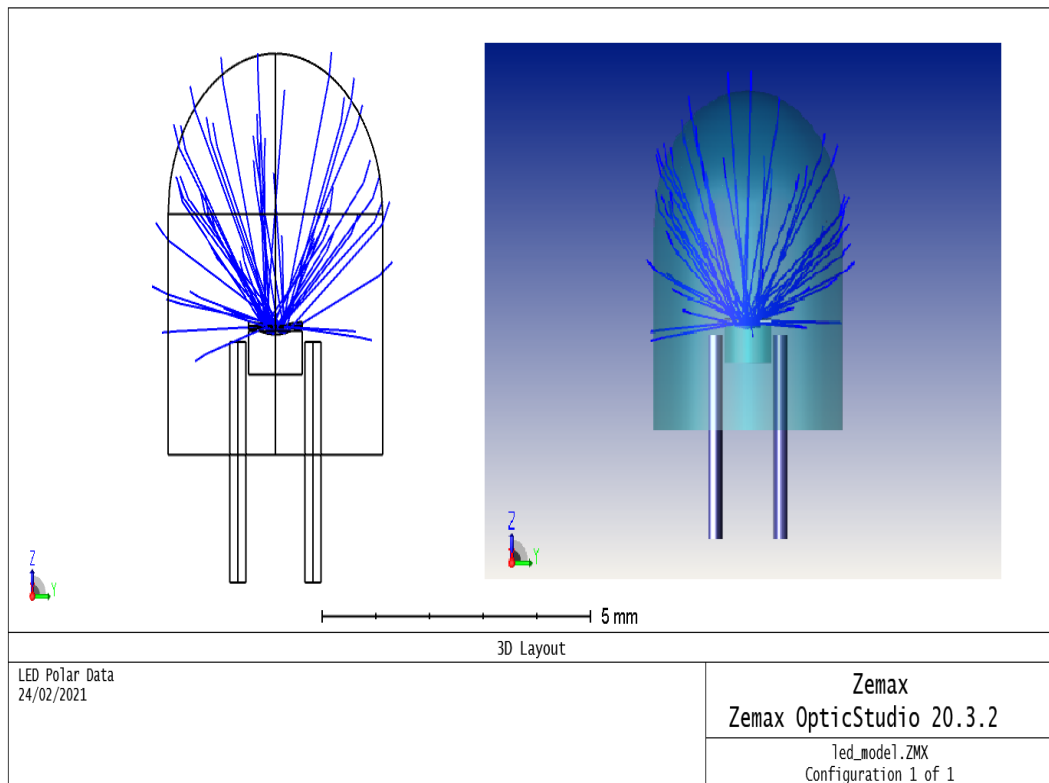
In the international market, the variety of LEDs available for sale is not negligible, and the types are mainly classified in terms of power and wavelength (ANNEX 3). In the present design, a generic light emitting diodes with a power of 3.6 W and a wavelength of 365 nm have been selected since several investigations have been reported in which these values are recommended due to the positive results obtained (see figure 19). In this sense, a wavelength of 365 nm, with an appropriate photocatalyst such as anatase, can trigger reactions such as oxidation of pharmaceutical compounds in water<sup>58</sup>, removal of bacteria<sup>59</sup>, oxidation of dyes<sup>60</sup>, and organic and inorganic compounds in general<sup>61</sup>. It is for these reasons that the photocatalyst used as model is anatase since it presents relatively low bandgap



energy (3.2 eV), and it has been reported that this semiconductor can be activated even at wavelengths longer than 400 nm.<sup>62</sup>

#### 4.1.1 Light source simulation

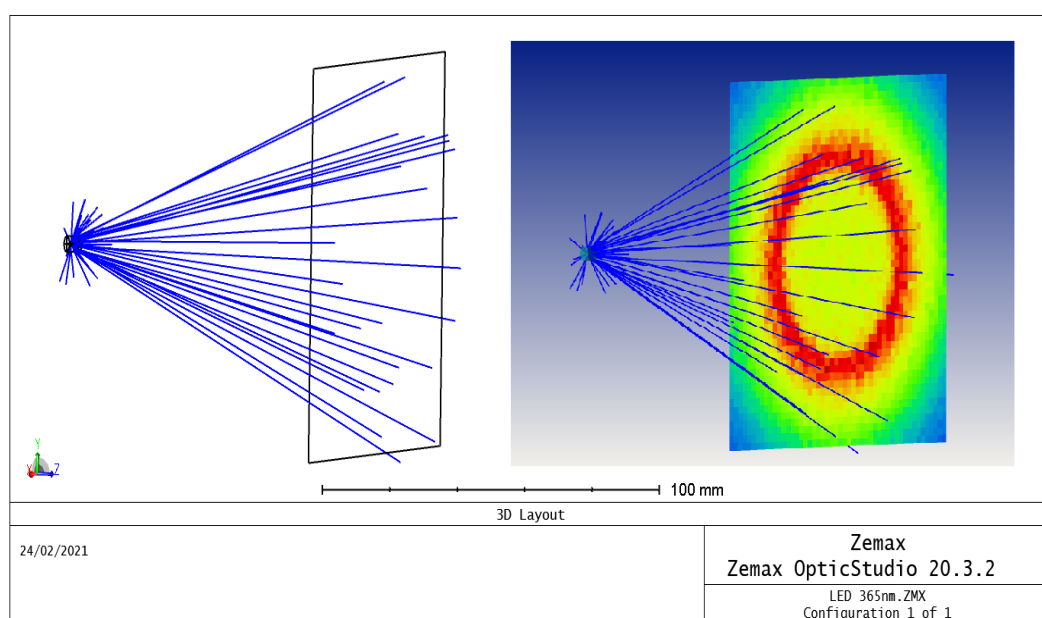
The software interface of OpticStudio by ZEMAX is very user friendly in terms of input data since it allows entering values such as the size of the structure, the number of beams to be used for the analysis, the power of the light source, the wavelength of the device, and the spatial location in three dimensions (see Chapter 3). Once all these values have been determined and entered, the simulator generates the associated physical structure and presents a model with real dimensions and defined spatial distribution (see Figure 20).



**Figure 20.** Simulation of a light emitting diode in OpticStudio.

Once the LED device is analyzed and complies with the specifications provided by the manufacturer, a receiver is simulated, which will be in charge of reading the information contained in the rays emitted from the source (see Figure 21). As stated in the mathematical basis of Chapter I, the magnitude of interest in

the system is called the received fluence ( $G$ ), whose units are  $W/m^2$  and represent the power of the photons of light per unit area on the surface of the source. In this context, the power required per unit area to activate a photocatalyst is called irradiance, which, in contrast with the fluence received, is quantified on the surface of the catalyst (receiver). It is important to emphasize that the proposed equipment must be able to work with different photocatalysts, which may require higher power, as shown in Table 2.



**Figure 21.** Drawing of 50 rays for an LED in Optic Studio.

**Table 2.** Irradiance for Photocatalyst Activation.

Photocatalyst	Irradiance ( $W/cm^2$ )	Reference
TiO <sub>2</sub> (Anatase)	0.0878	63, 1
CdTe	0.04	64
SrTiO <sub>3</sub>	0.1	65
Nb <sub>2</sub> O <sub>5</sub>	0.01	66

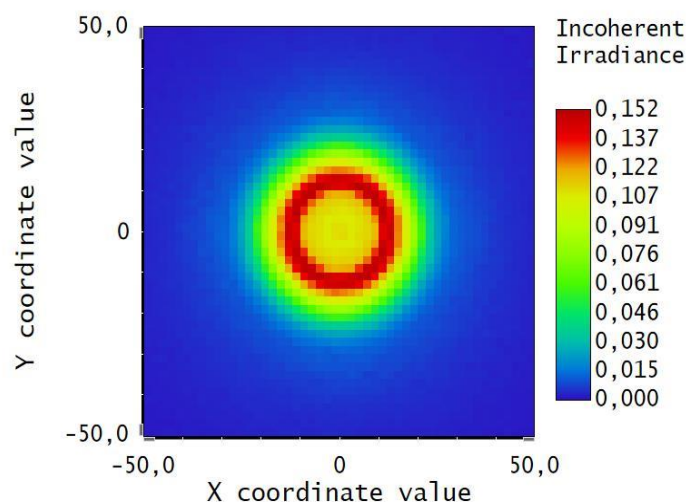
Based on the information reported, the equipment must work with an irradiance higher than  $0.1 \text{ W/cm}^2$  since this value belongs to one of the most complicated photocatalysts to activate in energetic terms ( $\text{SrTiO}_3$ ). Once the maximum irradiance value has been determined, the next step is to find the ideal distance between the source and the receiver to activate it.

#### **4.1.2 LED's distance**

The distance at which the source must be located from the surface of the photocatalyst is one of the most critical parameters of the whole system. Usually, this process is carried out experimentally, where the LEDs are placed at different distances from the receiver, and the irradiance obtained is measured. However, OpticStudio software allows the simulation of this experimental calculation to be performed with a high degree of accuracy.

Once the LED and the receiver have been simulated, the distance at which the receiver is to be located must be specified since the source is fixed. Then, we proceed to the ray tracing to obtain the graphical distribution of the power on the receiver. Simultaneously, the software calculates the irradiance on the surface of the receptor and generates the results using specific tables in units of  $\text{W/cm}^2$ . For the present experimentation, distances ranging from 30 cm to 100 cm were placed at intervals of 10 cm each (ANNEX 4).

It was determined that the appropriate distance at which the source should be placed from the surface of the photocatalyst is 40 cm or less (see Figure 22). This selection is because the photocatalyst that requires the highest irradiance is  $\text{SrTiO}_3$  with a value of  $0.1 \text{ W/cm}^2$  (see Table 2). Additionally, given that the system is designed with the objective of characterizing new photocatalysts, it is essential to exceed the aforementioned irradiance value in order to reduce as much as possible the energy limitations of the equipment in the event that the material to be characterized requires a more tremendous amount of energy. On the other hand, at distances of less than 40 cm, the energy parameters are met, but due to factors such as the volume of the sample holder and the catalyst support, these distances were discarded since they generated severe complications in the design.



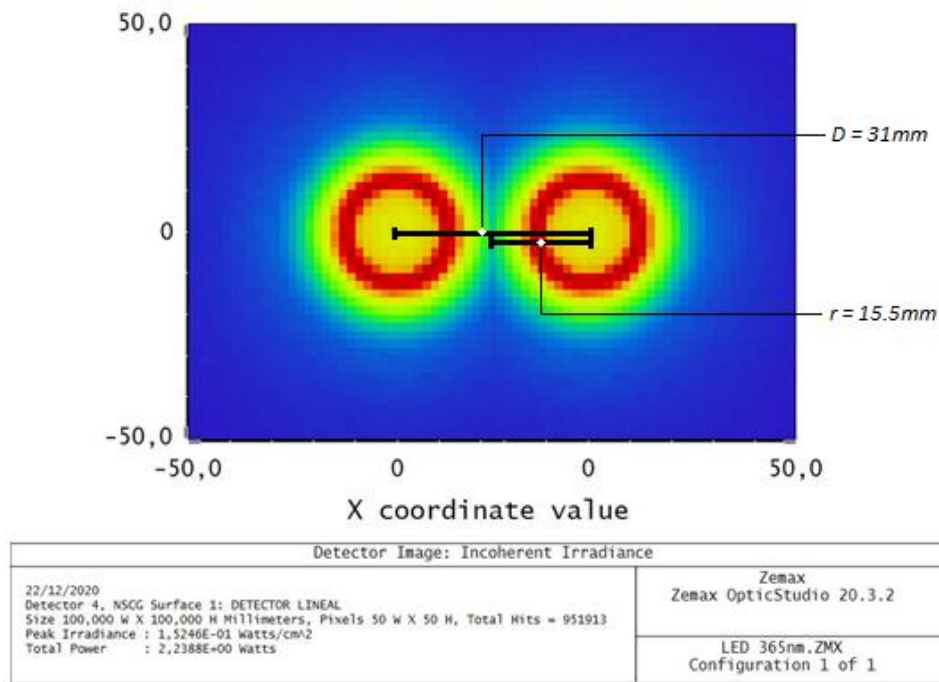
Detector Image: Incoherent Irradiance	
22/12/2020 Detector 4: NSCG Surface 1: DETECTOR LINEAL Size 100,000 W X 100,000 H Millimeters, Pixels 50 W X 50 H, Total Hits = 951913 Peak Irradiance : 1,5246E-01 Watts/cm <sup>2</sup> Total Power : 2,2388E+00 Watts	Zemax Zemax OpticStudio 20.3.2  LED 365nm.ZMX Configuration 1 of 1

**Figure 22.** Irradiance at a distance of 40 cm from the receptor.

#### 4.1.3 LED's distribution

Since the distance from the source has been determined, the next step is to determine the length at which one LED should be placed with respect to another. This value is of great importance since the homogeneity with which the sample is irradiated so that the whole system has uniform kinetics. On the other hand, this value allows determining the optimal amount of light emitting diodes needed for the equipment, resulting in an optimization of the system in economic and energetic terms. Additionally, by knowing the distance at which the light emitting diodes should be placed, it is possible to more accurately dimension values such as the volume of the sample holder, the volume of the samples, and the volume of the cylinder doped with the photocatalyst.

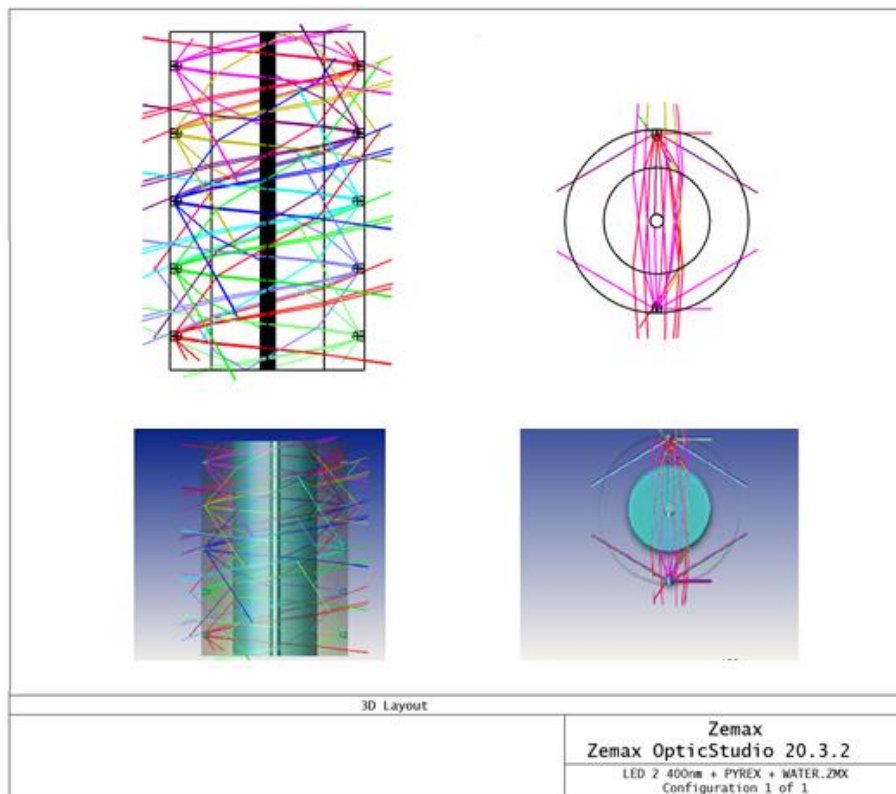
The magnitude of the distance that one LED should be from another can be calculated by the scale of the cone radiated by the source. As shown in Figure 21, the cone that presents the distribution has a diameter of 31 mm; therefore, the radius of the cone is set at 15.5 mm. Thus, from these values, it is determined that the distance at which two sources should be located is 31 mm with respect to one another, as shown in Figure 23.



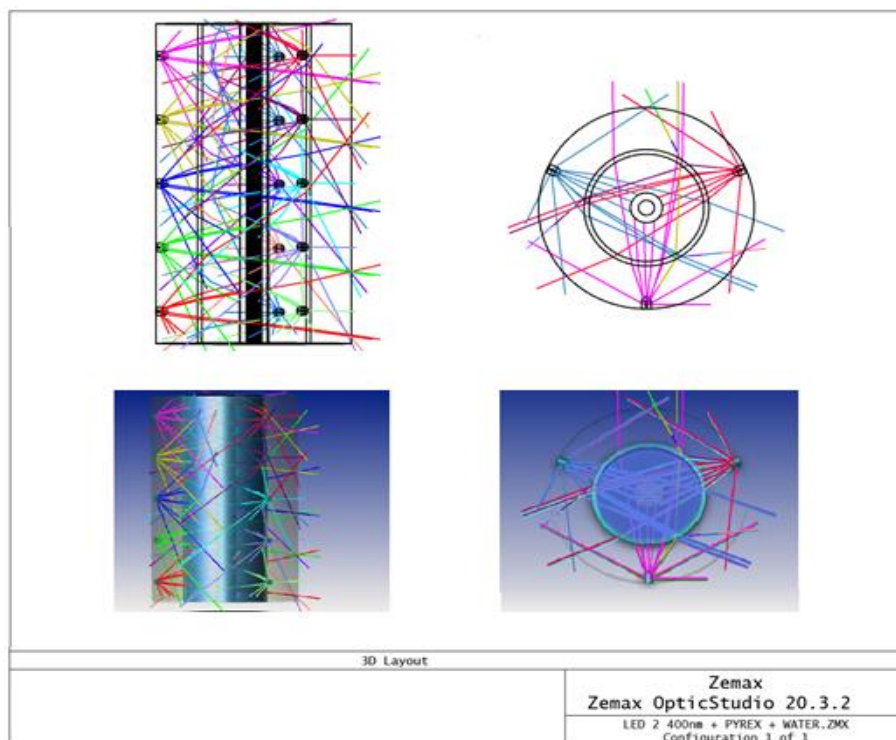
**Figure 23.** Distribution of 2 LEDs located at 10 cm from the surface.

The sample holder consists mainly of a 150 mm long Pyrex tube. Thus, it is necessary to place 5 LEDs for each row to irradiate the length of the specimen holder homogeneously, given that the maximum distance at which the LEDs should be separated is 31 mm.

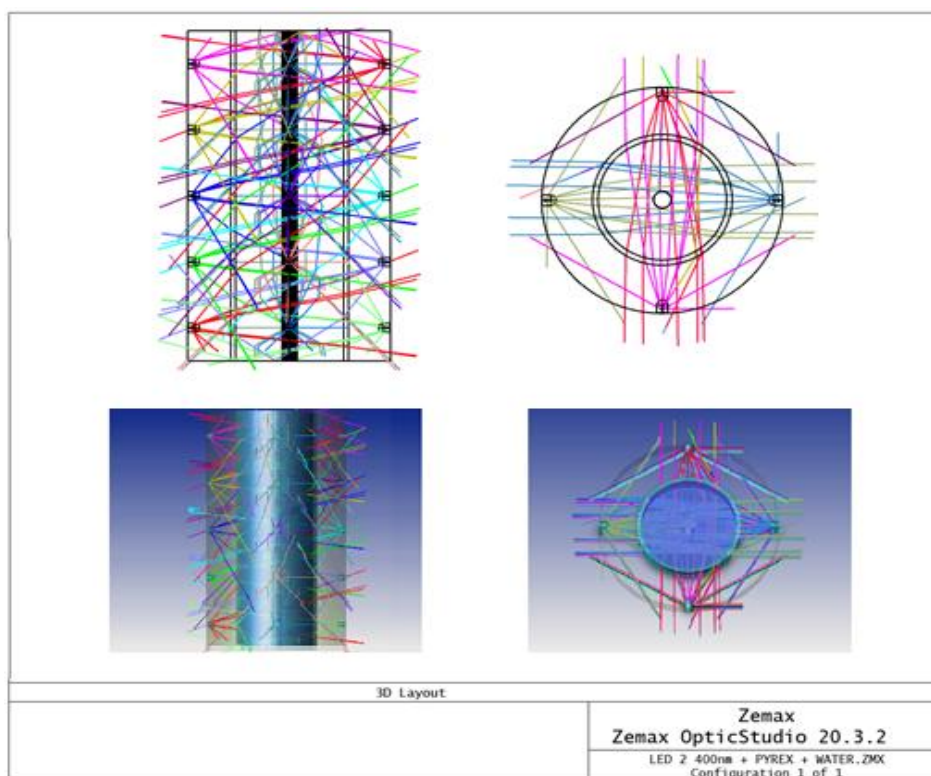
Next, it is necessary to determine the number of rows to be implemented to irradiate the entire external surface of the sample cylinder homogeneously. For this purpose, three distributions have been proposed. The first distribution contains two rows of LEDs, one in front of the other around the circumference (see Figure 24). The second distribution represented with three rows (see Figure 25), and the third distribution with four rows (see Figure 26).



**Figure 24.** Spatial distribution of two rows of 5 LEDs each.



**Figure 25.** Spatial distribution of three rows of 5 LEDs each.



**Figure 26.** Spatial distribution of four rows of 5 LEDs each.

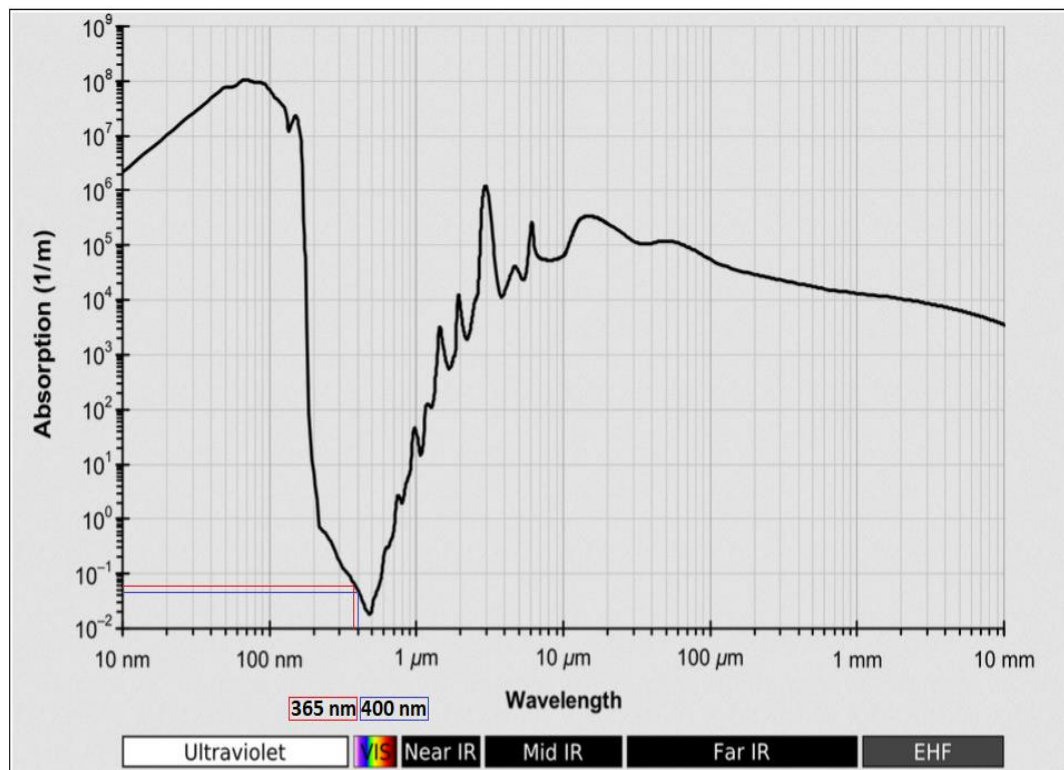
Additionally, in the photocatalytic reactor considered, the light beams emitted by the radiation source need to pass through certain materials to reach the surface of the photocatalyst. In this context, each light beam must pass through a Pyrex wall, followed by a wall of a particular fluid, which in this case is exemplified by water until it reaches the surface of the photocatalyst. According to the dimensions obtained from the commercial Pyrex tube, the wall thickness of the tube is 2 mm. Meanwhile, the water thickness is obtained from the subtraction between the inner radius of the Pyrex tube and the outer radius of the aluminum tube, taking into account that the latter must have the addition of the thickness of the anatase layer. This calculation results in a water thickness of 16 mm.

Once the indicated thickness has been placed on each material, the total Irradiance that would be reaching the surface of the catalyst is determined. It is important to emphasize that the system must work at a wavelength of 365 nm. However, this calculation cannot be carried out directly since the OpticStudio



simulator cannot work at less than 400nm when water is used as fluid due to inconveniences in the associated dispersion formula.

To solve this problem, an interpolation of the irradiance data obtained at 400 nm was carried out to determine the values required at 365 nm. To do this, it was first necessary to simulate at 400 nm without including the water wall, and then to contain the water wall to calculate the percentage variation of the values. Next, it is necessary to simulate at 365 nm without including the water wall, and with the previously obtained percentages, it was possible to get the required values at 365 nm. It is important to note that, as shown in Figure 27, this is possible since the absorption spectrum of water in the 365-400 nm range is extremely low ( $10^{-1}$ ), and therefore, it could be assumed that the variation of irradiance values in this interval is interpolable.

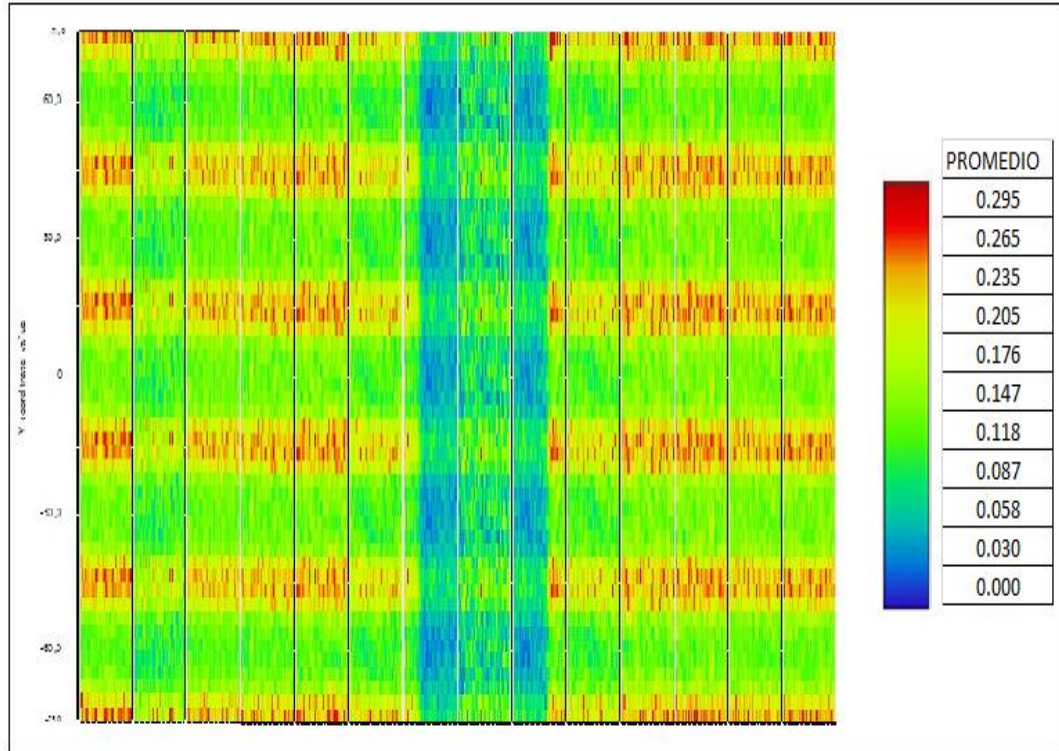


**Figure 27.** The absorption spectrum of liquid water.<sup>67, 68</sup>

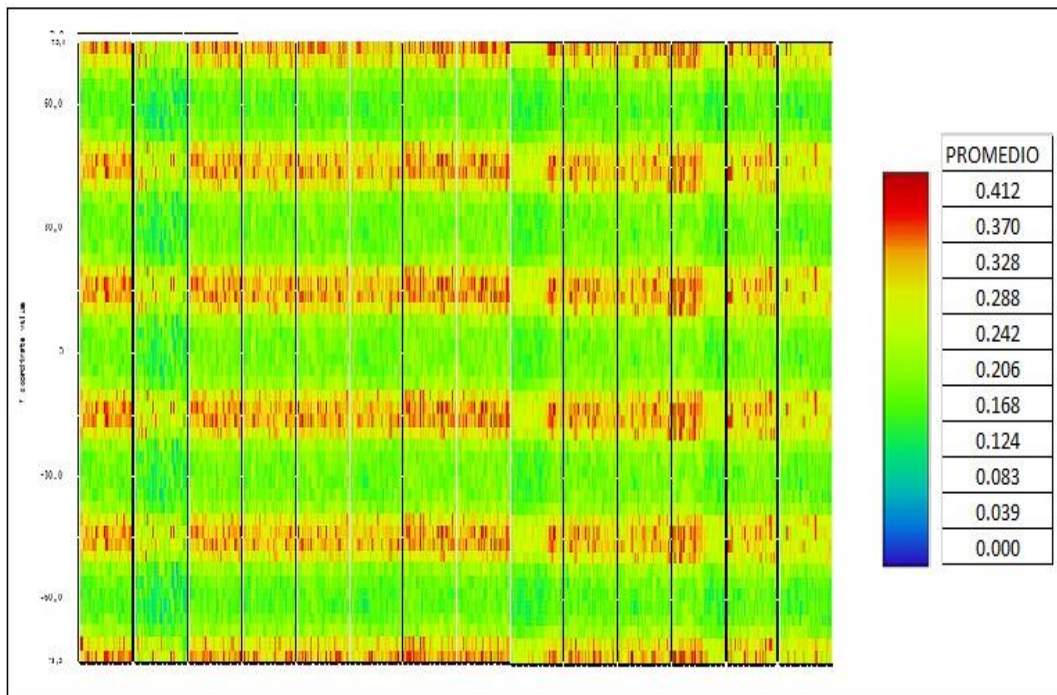
In this way, it is possible to determine both the irradiance in the system at the appropriate wavelength and the final distribution of the light radiation on the



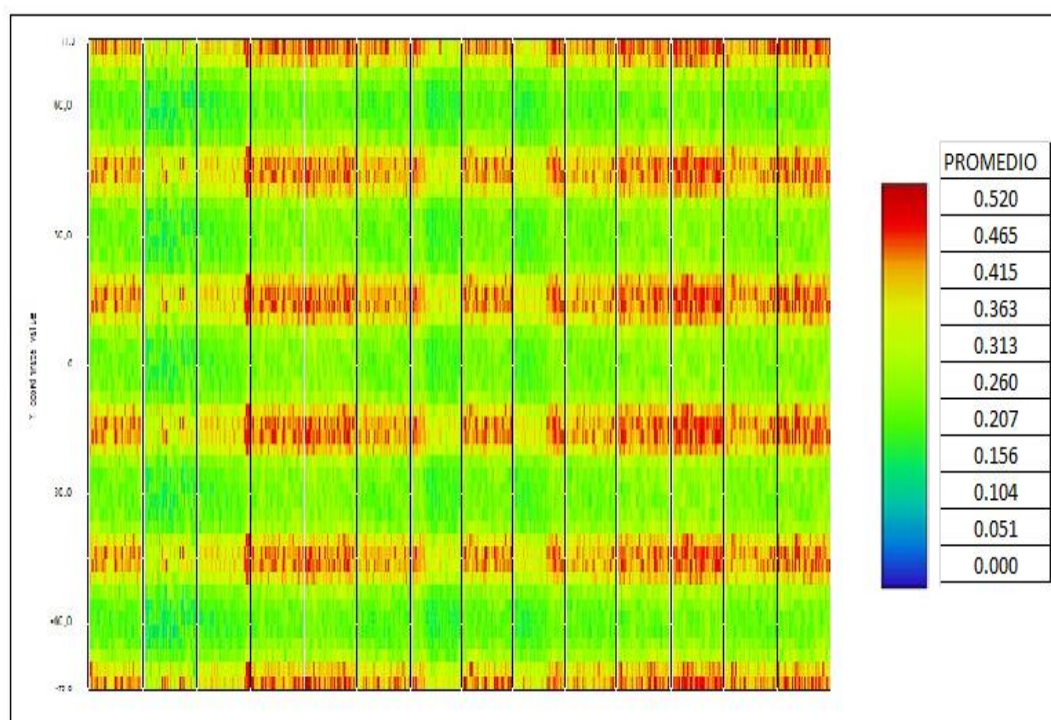
catalyst surface, as shown in Figures 28, 29 and 30 for two-row, three-row and four-row LED distribution.



**Figure 28.** Final irradiance in a distribution of two rows of 5 LEDs.



**Figure 29.** Final irradiance in the distribution of three rows of 5 LEDs.



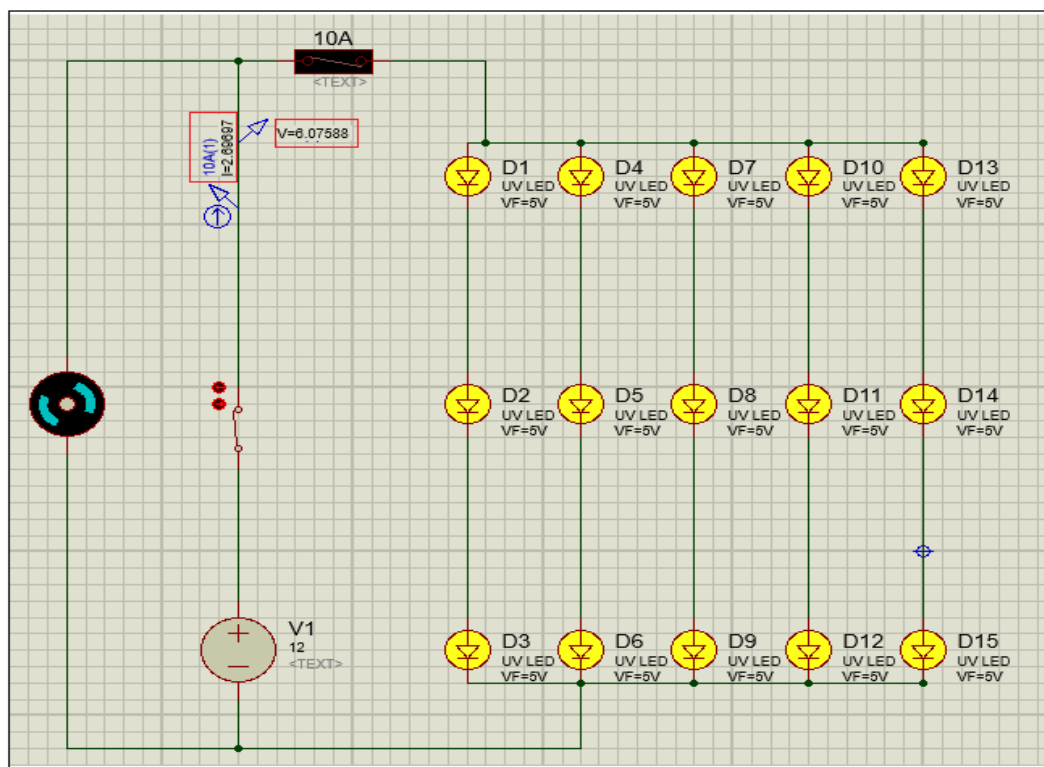
**Figure 30.** Final irradiance in the distribution of four rows of 5 LEDs.

It is determined that the best distribution for the present design is the one composed of three rows of five LEDs. This choice is mainly based on the irradiance values since the homogeneity is similar in the three cases. However, in terms of energy, the two-row distribution is not the best because its maximum peak is  $0.295 \text{ W/cm}^2$  and this relatively small value may be insufficient to activate certain new materials. In addition, the zones with the lowest energy for the three distributions have been taken into account. In this sense, the distribution composed of two rows of LEDs presents blue coloration zones, whose energy value does not exceed  $0.04 \text{ W/cm}^2$  and therefore this distribution would be not very efficient.

On the other hand, the distribution of four rows of LEDs is the one with the highest energy with a peak of  $0.52 \text{ W/cm}^2$ . However, when comparing this value with the maximum value of the distribution of three rows of LEDs, it is observed that there is a difference of  $0.108 \text{ W/cm}^2$ , which is not so remarkable if it requires increasing an entire row of five LEDs, thus affecting the economic feasibility.

## 4.2 Electrical circuit




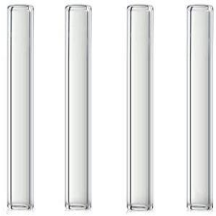


The electrical circuit required for the equipment is based on the aforementioned design criteria. In this context, the circuit must be able to power 15 LEDs and a stepper motor under the specifications of the manufacturer of these components to corroborate that the system is feasible and can be carried out physically. The Proteus 8 software was used for this task, which allows the simulation of the circuit, thus obtaining the values of voltage and amperage required by the system (Figure 31).







**Figure 31.** Circuit simulation in Proteus 8.

After the simulation, it is noted that to feed the circuit a voltage of 6.075 V and amperage of 2.696 A is necessary. These specifications allow to complete the values required for the search for components that are available for distribution and that meet the essential specifications (Table 3). Thus it is feasible to verify that the circuit can be built, and therefore the system is, from a theoretical aspect, fully functional.

**Table 3.** Components of the system.

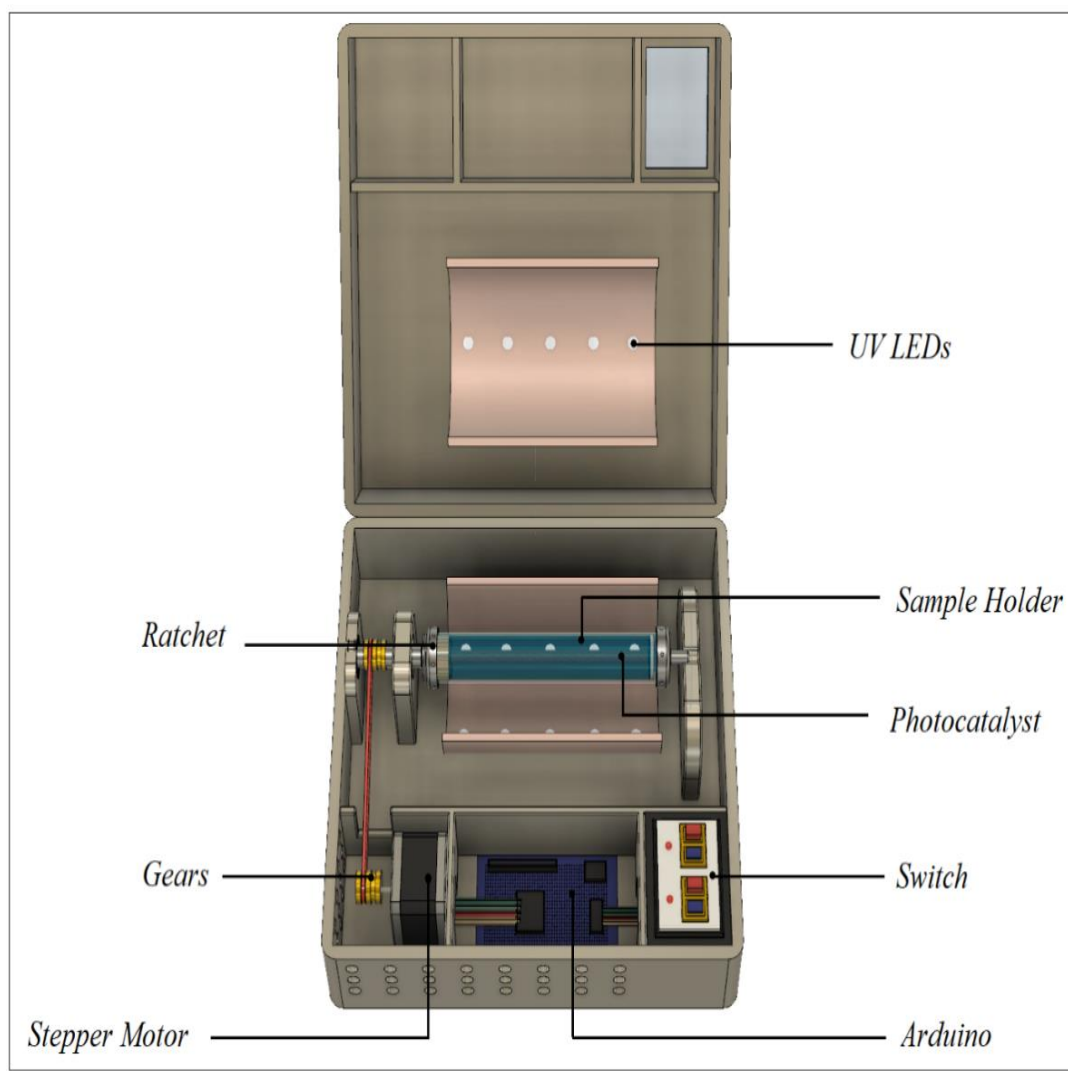
COMPONENT	CHARACTERISTICS	FIGURE
Light emitting diodes (LEDs)	<ol style="list-style-type: none"> <li>1. Dimensions: 5 mm</li> <li>2. Wavelength: 365 nm UV</li> <li>3. Voltaje: 5 V</li> <li>4. Power: 3.6 W</li> </ol>	
Aluminum pipe	<ol style="list-style-type: none"> <li>1. Dimensions: 6.4x130 mm</li> <li>2. Material: Aluminum</li> <li>3. Thickness: 2 mm</li> </ol>	
Copper pipe	<ol style="list-style-type: none"> <li>1. Dimensions: 45x150 mm</li> <li>2. Material: Copper</li> <li>3. Thickness: 1 mm</li> </ol>	
Pyrex glass (Sample holder) 55	<ol style="list-style-type: none"> <li>1. Dimensions: 25x150 mm</li> <li>2. Volume: 55 mL</li> <li>3. Transmission UV &gt; 90%</li> <li>4. Softening point: 820°C</li> <li>5. Transparent</li> </ol>	
Stepper motor	<ol style="list-style-type: none"> <li>1. Step angle: 1.8°</li> <li>2. Holding current: 1.7 A</li> <li>3. Phase resistance: 2.4 Ω</li> <li>4. Holding torque: 0.45 N.m</li> </ol>	
Switch	<ol style="list-style-type: none"> <li>1. Material: Metal / Plastic</li> <li>2. Dimensions: 15x30 mm</li> <li>3. Waterproof</li> <li>4. Color: Red</li> </ol>	

Ratchet	<ol style="list-style-type: none"> <li>1. Material: Steel CR-V</li> <li>2. Impact coupler</li> </ol>	
Arduino	<ol style="list-style-type: none"> <li>1. Dimensions: 17x15x4 cm</li> <li>2. Weight: 152 g</li> <li>3. Controller: ATmega328P</li> <li>4. Compatible: iOS/Windows</li> </ol>	
Source	<ol style="list-style-type: none"> <li>1. Dimensions: 20x18x5.4 cm</li> <li>2. Voltage: 12V</li> <li>3. Amperage: 10 A</li> <li>4. Power: 120 W</li> <li>5. Material: Aluminum</li> </ol>	
General structure (PETG)	<ol style="list-style-type: none"> <li>1. Melting Temperature: 91°C</li> <li>2. Insulator</li> <li>3. Recyclable</li> <li>4. Hardness: 1.41x10<sup>8</sup> Pa</li> </ol>	



### 4.3 Reactor structure

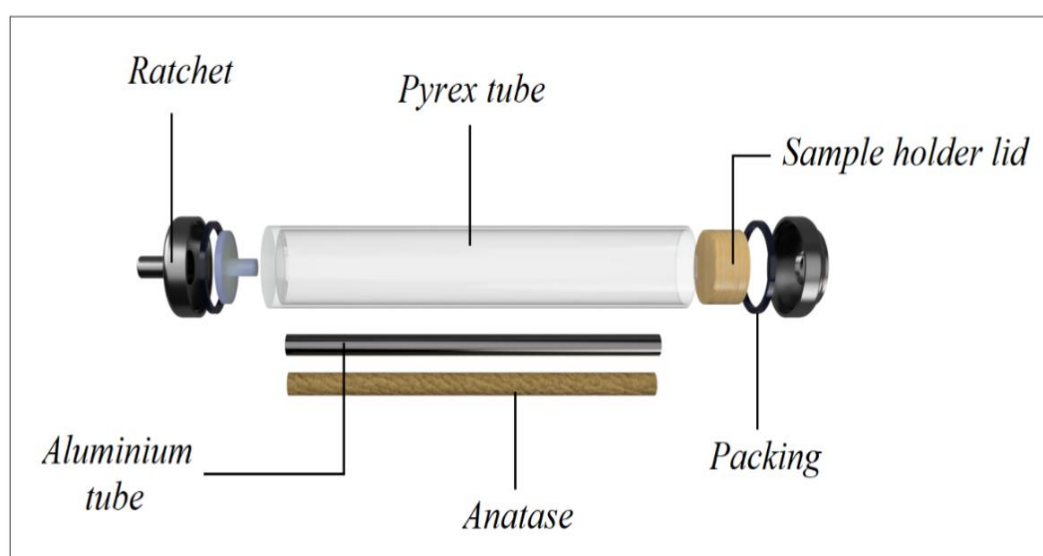
The modeling of the reactor structure was made in Autodesk Fusion 360 software, and three different virtual prototypes were tested and compared until the final design was reached (see Figure 32)



**Figure 32.** Final structure of the prototype is modeled in Autodesk Fusion 360.

The equipment is composed of an illumination system distributed in a cylindrical shape around the sample holder so that the illumination is as homogeneous as possible. The agitation of the system is performed by using a programmable stepper motor and a system of gears that drive the rotary motion to

the sample holder. The control system is equipped with two switches to turn on and off both the motor and the light source separately, thus extending the variety of experimental conditions. Next, the samples are placed inside a concentric Pyrex tube, at the ends of which there is a ratchet system connected to the aforementioned gear system, making it a completely removable system (see Figure 33). Finally, the catalyst is fixed on a concentric aluminum tube, whose surface has been previously oxidized to obtain the alumina support required for the system. The supported catalyst is located in the center of the whole system and is the last material to receive radiation from the source.



**Figure 33.** Sample holder ratchet system.

Once the 3D modeling and design process is completed, the rendering option can be applied to obtain a photorealistic image (see Figure 34), with which it is possible to get even closer to the physical design concept. It is important to emphasize that the system is fully portable, and therefore can be moved without the need to disassemble it, as shown in Figure 35.



**Figure 34.** Final structure of the prototype rendered in Autodesk Fusion 360.

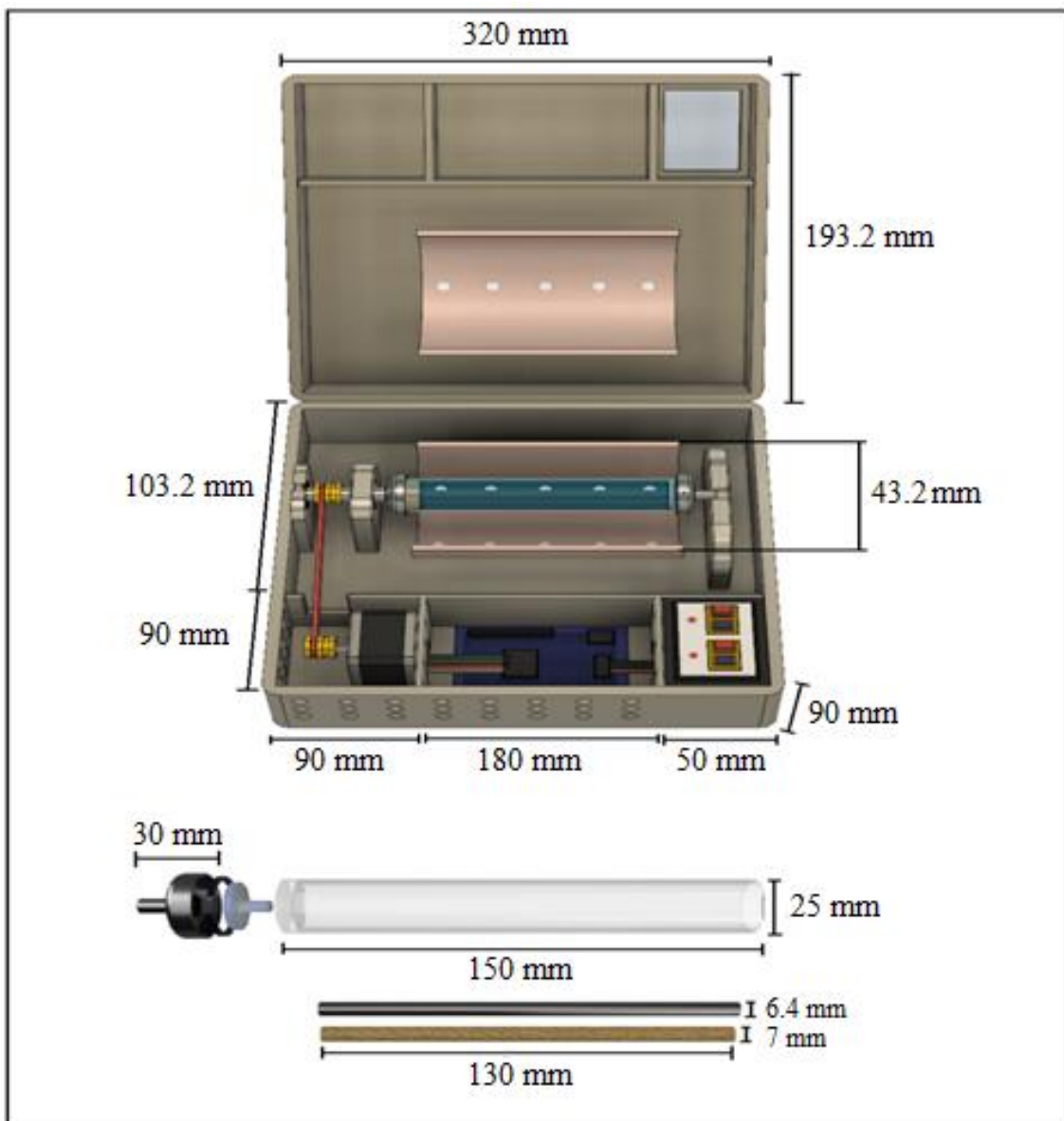


**Figure 35.** The final structure of the closed prototype.



#### 4.4 Equipment sizing

In this section, a compilation of all the data obtained to size the equipment is made. It is important to emphasize that the values have been generated thanks to the simulators and the materials available for the manufacture of the prototype. Figure 36 shows the final dimensions of the unit and its distribution according to the main design parameters.



**Figure 36.** Equipment sizing.

#### 4.5 Economic estimate (Class V)

A Class V economic estimate consists of developing a rough estimate of the monetary resources required to carry out the materialization of the prototype. For this purpose, a base or calculation criterion is established, which in this case has been proposed as three times the commercial value of each component. This parameter is based on the basis of covering expenses associated with time invested, factory defects of the products, research development and possible setbacks, thus generating the following results (see Table 4).

**Table 4.** Class V economical estimate.

Component	Retail cost (USD)	Final cost (USD)
Light emitting diodes (LEDs): 15 pcs	90	270
Aluminum pipe	11	33
Copper pipe	18	54
Pyrex glass	12	36
Switch: 2 pcs	10	30
Stepper motor	20	60
Ratchet	10	30
Arduino	15	45
Source	18	54
General Structure (PETG)	30	90
Assembly cost		230
		<b>932</b>

From the economic estimate based on the materials that are available for sale to the public, it can be determined that, in the first instance, a total of USD \$702 would be required to carry out the project. It is important to mention that this estimate may vary considerably as the prototype is developed.

## CONCLUSIONS AND RECOMMENDATIONS

The present study has allowed the design and modeling of a light-emitting diode based system for the characterization of materials with possible photocatalytic properties. The virtual prototype has three main features: the first and most important is the light source based on UV light emitting diodes working at a wavelength of 365 nm. The second feature is the way of implementing the photocatalyst, which for the design is supported on alumina, coming from an aluminum cylinder. It is important to emphasize that anatase was used as the photocatalyst to exemplify the calculations. However, the system will have to work with different types of materials. The last characteristic taken into account is the type of reactor to be used. In this context, it was decided to use a batch reactor due to essential advantages such as the sample volume and the high degree of conversion in the photocatalysis reactions.

The ZEMAX OpticStudio software was used to design the light source. With this program, it was obtained that the ideal distance at which the LEDs should be placed from the sample (photocatalyst) is 40 cm. In addition, the distance at which one LED should be set with respect to another is 31 mm, and finally, thanks to the irradiance data, it was determined that the best distribution for the light source in the system is in the form of three rows of LEDs with five units in each row. Thus, the total number of light-emitting diodes that are required for the equipment is 15 units.

Once the number of light-emitting diodes was determined, the design of the electrical circuit associated with the system was carried out. This must include both the LEDs and the motor that rotates the sample holder and homogenizes the irradiation. In this regard, it was obtained that the voltage required to power the circuit is 6.075 V, while the needed minimum amperage is 2.696 A. With this data, it is possible to find the necessary components to meet the manufacturing specifications of the equipment.

Finally, and thanks to the data obtained in the previous sections, it was possible to design and model the 3D prototype of the proposed system. For this purpose, the Autodesk Fusion 360 software was implemented, from which the design was obtained and later used for the final dimensioning.

---

## RECOMMENDATIONS

- The present study presents the design of a system for the characterization of materials with possible photocatalytic properties. For this purpose, the equipment consists of a batch reactor, in which the photocatalytic reactions are carried out. In this context, it is recommended to increase the number of reactors (ANNEX 5) in order to reduce the analysis time when dealing with a large number of materials. Additionally, this feature allows replicating the reactions under precisely the same conditions carried out at the same time.
- In order to make a physical prototype of the design carried out in this work, it is recommended to implement the same or similar materials to those mentioned in the previous sections. This is due to the fact that the bibliographic and analytical basis that supports this choice also decreases the probability of commissioning a device that is not functional and therefore does not meet the proposed objectives.
- With respect to the circuit design, it is recommended to improve the analysis of the power emitted from each light emitting diode. This in order to be able to control the amount of energy emitted from these LEDs and thus be able to vary this parameter depending on the objectives of the characterization.
- Finally, it is recommended to replicate the present design with photodiodes of different wavelengths. Especially in the visible light range. This with the objective of optimizing the system by verifying that it can work even if the source of light energy is the light emitted by the sun.

---

**BIBLIOGRAPHY**

1. Hashimoto, K., Irie, H. & Fujishima, A. TiO<sub>2</sub> photocatalysis: A historical overview and future prospects. *Japanese J. Appl. Physics, Part 1 Regul. Pap. Short Notes Rev. Pap.* **44**, 8269–8285 (2005).
  2. Pullerits, K. *et al.* Impact of UV irradiation at full scale on bacterial communities in drinking water. *npj Clean Water* **3**, 1–10 (2020).
  3. Fujishima, A., Rao, T. N. & Tryk, D. A. Titanium dioxide photocatalysis. *Journal of Photochemistry and Photobiology C: Photochemistry Reviews* (2000). doi:10.1016/S1389-5567(00)00002-2
  4. Braslavsky, S. E. *et al.* Glossary of terms used in photocatalysis and radiation catalysis (IUPAC recommendations 2011). *Pure Appl. Chem.* (2011). doi:10.1351/PAC-REC-09-09-36
  5. Malato, S., Fernández-Ibáñez, P., Maldonado, M. I., Blanco, J. & Gernjak, W. Decontamination and disinfection of water by solar photocatalysis: Recent overview and trends. *Catalysis Today* (2009). doi:10.1016/j.cattod.2009.06.018
  6. Doyle, R. L., Godwin, I. J., Brandon, M. P. & Lyons, M. E. G. Redox and electrochemical water splitting catalytic properties of hydrated metal oxide modified electrodes. *Physical Chemistry Chemical Physics* (2013). doi:10.1039/c3cp51213d
  7. Ibhaddon, A. O. & Fitzpatrick, P. Heterogeneous photocatalysis: Recent advances and applications. *Catalysts* **3**, 189–218 (2013).
  8. Simonsen, M. E. Heterogeneous Photocatalysis. in *Chemistry of Advanced Environmental Purification Processes of Water: Fundamentals and Applications* (2014). doi:10.1016/B978-0-444-53178-0.00004-3
  9. Augugliaro, V., Palmisano, G., Palmisano, L. & Soria, J. Heterogeneous photocatalysis and catalysis: An overview of their distinctive features. *Heterog. Photocatal. Relationships with Heterog. Catal. Perspect.* 1–24 (2019). doi:10.1016/B978-0-444-64015-4.00001-8
  10. Raupp, G. B. & Junio, C. T. Photocatalytic oxidation of oxygenated air toxics.
-

- Appl. Surf. Sci.* **72**, 321–327 (1993).
11. Grčić, I., Vrsaljko, D., Katančić, Z. & Papić, S. Purification of household greywater loaded with hair colorants by solar photocatalysis using TiO<sub>2</sub>-coated textile fibers coupled flocculation with chitosan. *J. Water Process Eng.* **5**, 15–27 (2015).
  12. Khan, M. M., Adil, S. F. & Al-Mayouf, A. Metal oxides as photocatalysts. *J. Saudi Chem. Soc.* **19**, 462–464 (2015).
  13. Hernández-Ramírez, A. & Medina-Ramírez, I. *Photocatalytic semiconductors: Synthesis, characterization, and environmental applications. Photocatalytic Semiconductors: Synthesis, Characterization, and Environmental Applications* (2015). doi:10.1007/978-3-319-10999-2
  14. Sundar, K. P. & Kanmani, S. Progression of Photocatalytic reactors and its comparison: A Review. *Chem. Eng. Res. Des.* **154**, 135–150 (2020).
  15. Bickley, R. I., Slater, M. J. & Wang, W. J. Engineering development of a photocatalytic reactor for waste water treatment. *Process Saf. Environ. Prot.* (2005). doi:10.1205/psep.04028
  16. Baly, E. C. C., Heilbron, I. M. & Barker, W. F. CX. - Photocatalysis. Part I. The synthesis of formaldehyde and carbohydrates from carbon dioxide and water. *J. Chem. Soc. Trans.* (1921). doi:10.1039/CT9211901025
  17. Chatterjee, D. & Dasgupta, S. Visible light induced photocatalytic degradation of organic pollutants. *J. Photochem. Photobiol. C Photochem. Rev.* **6**, 186–205 (2005).
  18. Saravanan, R., Gracia, F. & Stephen, A. Basic Principles, Mechanism, and Challenges of Photocatalysis. in (2017). doi:10.1007/978-3-319-62446-4\_2
  19. Peiris, J. S. M., Guan, Y. & Yuen, K. Y. Severe acute respiratory syndrome. *Nature Medicine* (2004). doi:10.1038/nm1143
  20. Yuan, Q. *et al.* Selective Adsorption and Photocatalytic Degradation of Extracellular Antibiotic Resistance Genes by Molecularly-Imprinted Graphitic Carbon Nitride. *Environ. Sci. Technol.* (2020). doi:10.1021/acs.est.9b06926
-

- 
21. Achour S & Chabbi F. Disinfection of Drinking Water-Constraints and Optimization Perspectives in Algeria. *Larhyss J. Larhyss/Journal n° Achour F. Chabbi / Larhyss J.* (2014).
  22. Asahi, R., Morikawa, T., Ohwaki, T., Aoki, K. & Taga, Y. Visible-light photocatalysis in nitrogen-doped titanium oxides. *Science* (80-. ). (2001). doi:10.1126/science.1061051
  23. Kim, S. *et al.* Evaluation of performance with small and scale-up rotating and flat reactors; photocatalytic degradation of bisphenol A, 17B–estradiol, and 17A–ethynyl estradiol under solar irradiation. *J. Hazard. Mater.* (2017). doi:10.1016/j.jhazmat.2017.04.047
  24. Chatterjee, D. & Dasgupta, S. Visible light induced photocatalytic degradation of organic pollutants. *Journal of Photochemistry and Photobiology C: Photochemistry Reviews* (2005). doi:10.1016/j.jphotochemrev.2005.09.001
  25. Liu, B., Zhao, X., Terashima, C., Fujishima, A. & Nakata, K. Thermodynamic and kinetic analysis of heterogeneous photocatalysis for semiconductor systems. *Physical Chemistry Chemical Physics* (2014). doi:10.1039/c3cp55317e
  26. Yoon, T. P., Ischay, M. A. & Du, J. Visible light photocatalysis as a greener approach to photochemical synthesis. *Nat. Chem.* (2010). doi:10.1038/nchem.687
  27. Guo, Q., Zhou, C., Ma, Z. & Yang, X. Fundamentals of TiO<sub>2</sub> Photocatalysis: Concepts, Mechanisms, and Challenges. *Advanced Materials* (2019). doi:10.1002/adma.201901997
  28. Opezzo, O. J., Costa, C. S. & Pizarro, R. A. Effects of ultraviolet A radiation on survival and growth of Gram negative bacteria . Effects of ultraviolet A radiation on survival and growth of Gram negative bacteria. *Trends Photochem. Photobiol.* **13**, 2–15 (2011).
  29. Casado, C. *et al.* Design and validation of a LED-based high intensity photocatalytic reactor for quantifying activity measurements. *Chem. Eng. J.* **327**, 1043–1055 (2017).
  30. Bouchy, M. & Zahraa, O. Photocatalytic reactors. *Int. J. Photoenergy* **5**, 191–197
-

- (2003).
31. Yasmina, M., Mourad, K., Mohammed, S. H. & Khaoula, C. Treatment heterogeneous photocatalysis; Factors influencing the photocatalytic degradation by TiO<sub>2</sub>. *Energy Procedia* **50**, 559–566 (2014).
  32. Khodadadian, F. *et al.* Design, characterization and model validation of a LED-based photocatalytic reactor for gas phase applications. *Chem. Eng. J.* **333**, 456–466 (2018).
  33. Jo, W. K. & Tayade, R. J. New generation energy-efficient light source for photocatalysis: LEDs for environmental applications. *Industrial and Engineering Chemistry Research* (2014). doi:10.1021/ie404176g
  34. Minnett, P. J., Fox, N. & Wimmer, W. *Optical Radiometry for Ocean Climate Measurements. Academic press* (2014).
  35. Raithby, G. D. Evaluation of discretization errors in finite-volume radiant heat transfer predictions. *Numer. Heat Transf. Part B Fundam.* (1999). doi:10.1080/104077999275631
  36. Sommer, R. *et al.* Inactivation of bacteriophages in water by means of non-ionizing (UV-253.7nm) and ionizing (gamma) radiation: A comparative approach. *Water Res.* (2001). doi:10.1016/S0043-1354(01)00030-6
  37. Elyasi, S. Development of Uv Photoreactor Models for water treatment. (2009).
  38. Gilbert-Kawai, E., Wittenberg, M., Gilbert-Kawai, E. & Wittenberg, M. Beer–Lambert law. in *Essential Equations for Anaesthesia* (2014). doi:10.1017/cbo9781139565387.023
  39. Singh, S. Refractive Index Measurement and its Applications. *Phys. Scr.* **65**, 167–180 (2002).
  40. Kovalenko, S. A. Descartes-Snell law of refraction with absorption. *Semicond. Physics, Quantum Electron. Optoelectron.* (2001). doi:10.15407/spqeo4.03.214
  41. Onishi, T. & Onishi, T. Photocatalyst. in *Quantum Computational Chemistry* (2018). doi:10.1007/978-981-10-5933-9\_12
  42. Rincón, A. G. & Pulgarin, C. Photocatalytical inactivation of E. coli: Effect of
-



- (continuous-intermittent) light intensity and of (suspended-fixed) TiO<sub>2</sub> concentration. *Appl. Catal. B Environ.* (2003). doi:10.1016/S0926-3373(03)00076-6
43. Byrne, C., Subramanian, G. & Pillai, S. C. Recent advances in photocatalysis for environmental applications. *J. Environ. Chem. Eng.* (2018). doi:10.1016/j.jece.2017.07.080
  44. Chen, X. & Mao, S. S. Titanium dioxide nanomaterials: Synthesis, properties, modifications and applications. *Chemical Reviews* (2007). doi:10.1021/cr0500535
  45. Reddy, K. M., Manorama, S. V. & Reddy, A. R. Bandgap studies on anatase titanium dioxide nanoparticles. *Mater. Chem. Phys.* (2003). doi:10.1016/S0254-0584(02)00343-7
  46. Xu, Y. & Langford, C. H. Enhanced photoactivity of a titanium(IV) oxide supported on ZSM5 and zeolite A at low coverage. *J. Phys. Chem.* (1995). doi:10.1021/j100029a031
  47. Curcio, M. S., Oliveira, M. P., Waldman, W. R., Sánchez, B. & Canela, M. C. TiO<sub>2</sub> sol-gel for formaldehyde photodegradation using polymeric support: photocatalysis efficiency versus material stability. *Environ. Sci. Pollut. Res.* (2015). doi:10.1007/s11356-014-2683-4
  48. Habibpanah, A. A., Pourhashem, S. & Sarpoolaky, H. Preparation and characterization of photocatalytic titania-alumina composite membranes by sol-gel methods. *J. Eur. Ceram. Soc.* (2011). doi:10.1016/j.jeurceramsoc.2011.06.014
  49. WATARAI, S. Chemical Reactor. *J. Soc. Mech. Eng.* (1965). doi:10.1299/jsmemag.68.559\_1020
  50. Ding, J., Wang, X., Zhou, X. F., Ren, N. Q. & Guo, W. Q. CFD optimization of continuous stirred-tank (CSTR) reactor for biohydrogen production. *Bioresour. Technol.* (2010). doi:10.1016/j.biortech.2010.03.146
  51. Theodore, L. Continuous Stirred Tank Reactors. in *Chemical Reactor Analysis and Applications for the Practicing Engineer* (2012). doi:10.1002/9781118158630.ch9
  52. Liu, S. Batch Reactor. in *Bioprocess Engineering* (2017). doi:10.1016/b978-0-
-

- 444-63783-3.00004-6
53. Karer, G. & Škrjanc, I. Batch reactor. *Stud. Comput. Intell.* (2013). doi:10.1007/978-3-642-33947-9\_6
  54. Luyben, W. L. *Chemical Reactor Design and Control. Chemical Reactor Design and Control* (2006). doi:10.1002/9780470134917
  55. Lukes, P., Clupek, M., Babicky, V. & Sunka, P. Ultraviolet radiation from the pulsed corona discharge in water. *Plasma Sources Sci. Technol.* **17**, (2008).
  56. Bakin, N. N., Tuyev, V. I. & Yauk, E. F. LED lighting. in *12th International Conference and Seminar on Micro/Nanotechnologies and Electron Devices, EDM'2011 - Proceedings* (2011). doi:10.1109/EDM.2011.6006944
  57. Massa, G. D., Kim, H. H., Wheeler, R. M. & Mitchell, C. A. Plant productivity in response to LED lighting. in *HortScience* (2008). doi:10.21273/hortsci.43.7.1951
  58. Rodríguez, E. M. *et al.* Mechanism considerations for photocatalytic oxidation, ozonation and photocatalytic ozonation of some pharmaceutical compounds in water. *J. Environ. Manage.* (2013). doi:10.1016/j.jenvman.2013.04.024
  59. He, Q., Zhang, Y., Cai, X. & Wang, S. Fabrication of gelatin-TiO<sub>2</sub> nanocomposite film and its structural, antibacterial and physical properties. *Int. J. Biol. Macromol.* (2016). doi:10.1016/j.ijbiomac.2015.12.012
  60. Assaad, A., Pontvianne, S. & Pons, M. N. Photodegradation-based detection of fluorescent whitening agents in a mountain river. *Chemosphere* (2014). doi:10.1016/j.chemosphere.2013.12.095
  61. Altin, I. & Sökmen, M. Preparation of TiO<sub>2</sub>-polystyrene photocatalyst from waste material and its usability for removal of various pollutants. *Appl. Catal. B Environ.* (2014). doi:10.1016/j.apcatb.2013.06.014
  62. Sacco, O., Sannino, D. & Vaiano, V. Packed bed photoreactor for the removal of water pollutants using visible light emitting diodes. *Appl. Sci.* (2019). doi:10.3390/app9030472
  63. González-Burciaga, L. A. *et al.* Characterization and comparative performance of TiO<sub>2</sub> photocatalysts on 6-mercaptopurine degradation by solar heterogeneous
-

- photocatalysis. *Catalysts* **10**, (2020).
64. Bätzner, D. L., Romeo, A., Zogg, H. & Tiwari, A. N. CdTe/CdS Solar Cell Performance under Low Irradiance. *Proc. 17th Eur. Photovolt. Sol. Energy Conf. Exhib.* **1**, 1180–1183 (2002).
  65. Hara, T., Ishiguro, T. & Shinozaki, K. Ultraviolet-light-induced desorption of oxygen from srTiO<sub>3</sub> surfaces. *Jpn. J. Appl. Phys.* **50**, (2011).
  66. Guo, P. & Aegerter, M. A. RU(II) sensitized Nb<sub>2</sub>O<sub>5</sub> solar cell made by the sol-gel process. *Thin Solid Films* (1999). doi:10.1016/S0040-6090(99)00215-1
  67. Pope, R. M. & Fry, E. S. Absorption spectrum (380–700 nm) of pure water II Integrating cavity measurements. *Appl. Opt.* (1997). doi:10.1364/ao.36.008710
  68. Mason, J. D., Cone, M. T. & Fry, E. S. Ultraviolet (250–550 nm) absorption spectrum of pure water. *Appl. Opt.* (2016). doi:10.1364/ao.55.007163

# ANNEX

**ANNEX 1. Source for ZEMAX OpticStudio software download.**

Zemax

CONTACT US SEARCH CUSTOMER LOG-IN

PRODUCTS CUSTOMER SUCCESS APPLICATIONS RESOURCES TRAINING PRICING PROGRAMS BLOG

Products > OpticStudio > Request a Trial

## Try OpticStudio for free!

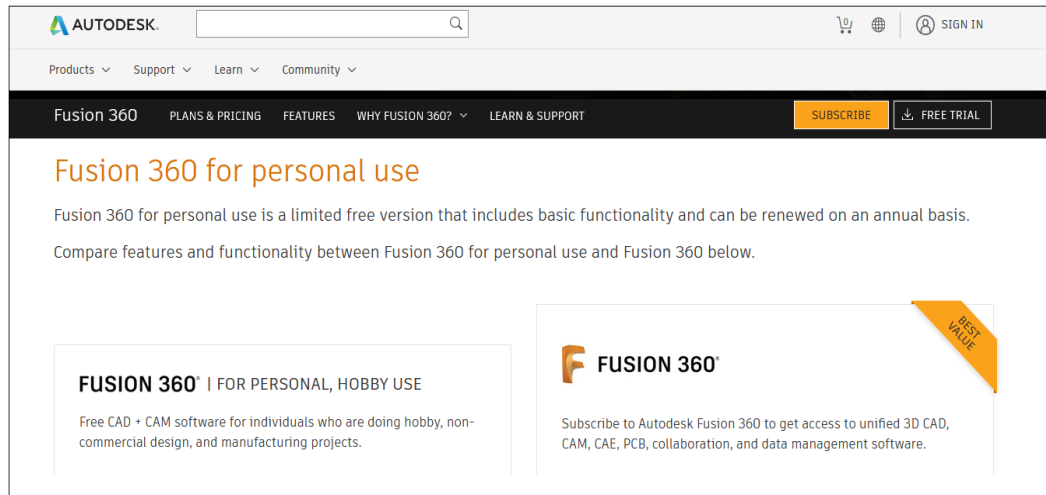
OpticStudio combines complex physics and interactive visuals so you can analyze, simulate, and optimize optics, lighting and illumination systems, and laser systems, all within tolerance specifications. Top companies in aerospace, astronomy, automotive, biomedical research, consumer electronics, and machine vision all rely on OpticStudio to create cutting-edge products.

Please fill out the optical design software trial request form. We will get in touch to provide you with access to your free OpticStudio trial.

If you are a student or educator, [click here](#)



<https://www.zemax.com/products/opticstudio/requestatrial>

**ANNEX 2.** Source for Autodesk Fusion 360 software download.

The screenshot displays the Autodesk website's product page for Fusion 360. The top navigation bar includes the Autodesk logo, a search bar, and links for 'SIGN IN', 'PRODUCTS', 'SUPPORT', 'LEARN', and 'COMMUNITY'. A secondary navigation bar features 'Fusion 360', 'PLANS & PRICING', 'FEATURES', 'WHY FUSION 360?', and 'LEARN & SUPPORT', along with 'SUBSCRIBE' and 'FREE TRIAL' buttons. The main content area is titled 'Fusion 360 for personal use' and describes it as a limited free version. Below this, two columns compare the 'FUSION 360 | FOR PERSONAL, HOBBY USE' (free software for hobbyists) with the 'FUSION 360' (full subscription software). A 'BEST VALUE' badge is placed over the full version's box.


<https://www.autodesk.com/products/fusion-360/personal>

**ANNEX 3. Listing of UV LEDs for Commercial Distribution.**

**Technical Details**

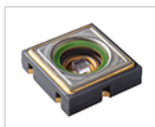
**5mm 365nm UV LED Ultra Violet led**

Item Weight	0.64 ounces
Package Dimensions	39.37 x 39.37 x 19.69 inches
Size	5mm
Style	Classic
Shape	Bulb
Power Source	Battery-powered
Voltage	5 Volts
Wattage	3.6 watts
Type of Bulb	LED
Special Features	Low Power Consumption



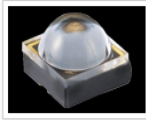

(Ts=25°C)

Part No.	NCSU434A <span style="color: red;">N</span>	
Peak Wavelength $\lambda_p$	Typ.(nm)	280
Radiant Flux $\Phi_E$	Typ.(mW)	17.5
Forward Voltage $V_F$	Typ.(V)	5.3
	Max.(V)	6.0
Directivity $2\theta_{1/2}$	Typ.(degree)	110
$I_F$	(mA)	100
Size	LxWxH (mm)	3.5x3.5x1.72



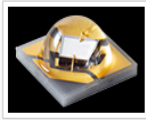
(Ts=25°C)

Part No.	NCSU334B <span style="color: red;">N</span>	
Peak Wavelength $\lambda_p$	Typ.(nm)	280
Radiant Flux $\Phi_E$	Typ.(mW)	70
Forward Voltage $V_F$	Typ.(V)	5.5
	Max.(V)	6.5
Directivity $2\theta_{1/2}$	Typ.(degree)	115
$I_F$	(mA)	350
Size	LxWxH (mm)	6.8x6.8x2.12

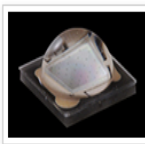


(Ts=25°C)

Part No.		NVSU233B-D4			
Peak Wavelength $\lambda_p$	Typ.(nm)	365	385	395	405
Radiant Flux $\Phi_E$	Typ.(mW)	1,450	1,730	1,650	1,400
Forward Voltage $V_F$	Typ.(V)	3.85	3.7	3.65	3.45
	Max.(V)	4.2		4.0	
Directivity $2\theta_{1/2}$	Typ.(degree)	60			
$I_F$	(mA)	1,000			
Size	LxWxH (mm)	3.5x3.5x2.73			



Part No.		NCSU276C	
Peak Wavelength $\lambda_p$	Typ.(nm)	365	
Radiant Flux $\Phi_E$	Typ.(mW)	1,050	
Forward Voltage $V_F$	Typ.(V)	3.8	
	Max.(V)	4.4	
Directivity $2\theta_{1/2}$	Typ.(degree)	120	
$I_F$	(mA)	500	
Size	LxWxH (mm)	3.5x3.5x2.0	



(Ts=25°C)

Part No.		NVSU119C			
Peak Wavelength $\lambda_p$	Typ.(nm)	375	385	395	405
Radiant Flux $\Phi_E$	Typ.(mW)	1,160	1,450	1,450	1,420
Forward Voltage $V_F$	Typ.(V)	3.4	3.35	3.3	3.1
	Max.(V)	3.8			3.6
Directivity $2\theta_{1/2}$	Typ.(degree)	135			140
$I_F$	(mA)	700			
Size	LxWxH (mm)	3.5x3.5x2.0			

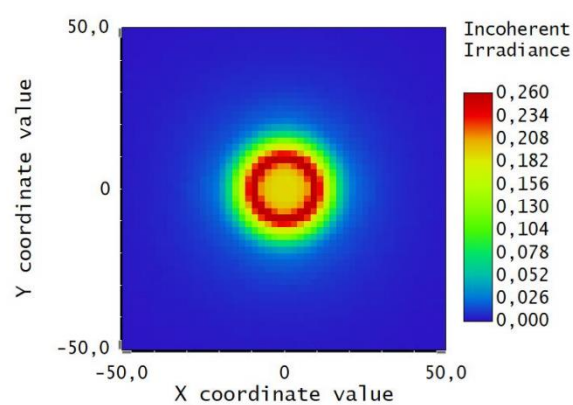
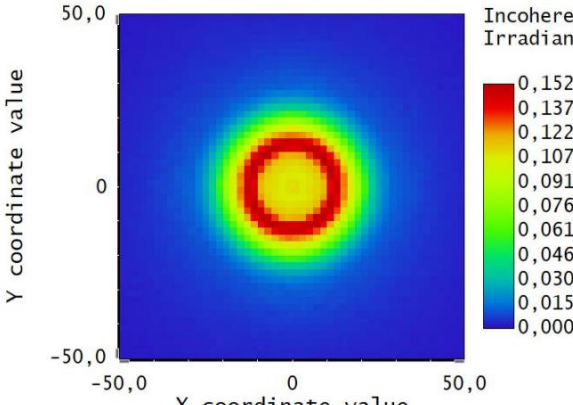
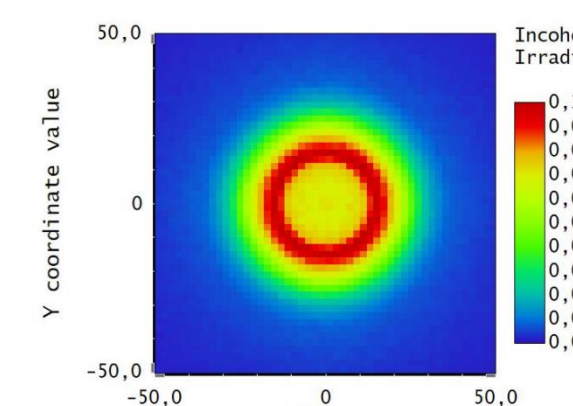


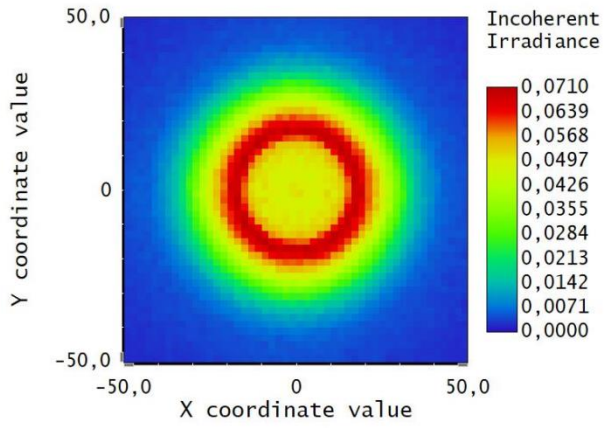
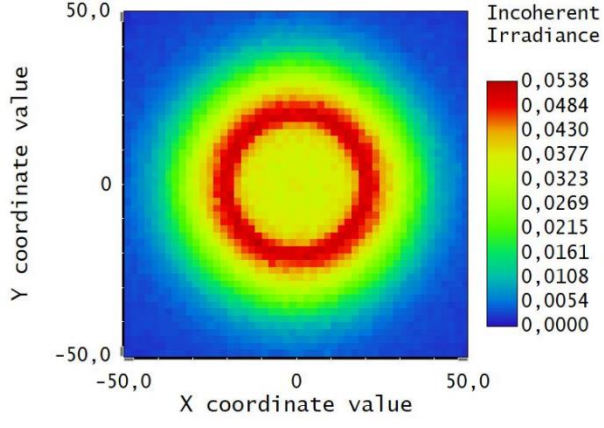
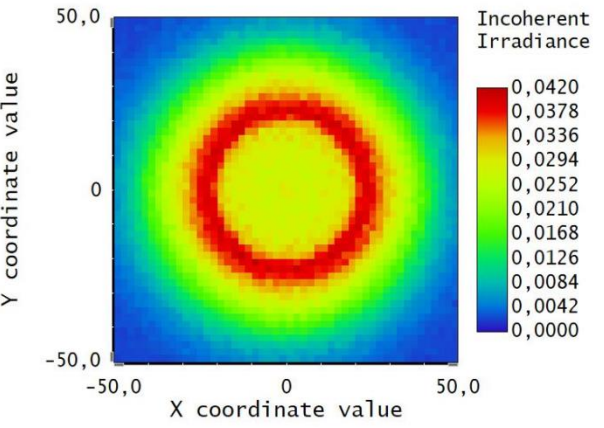


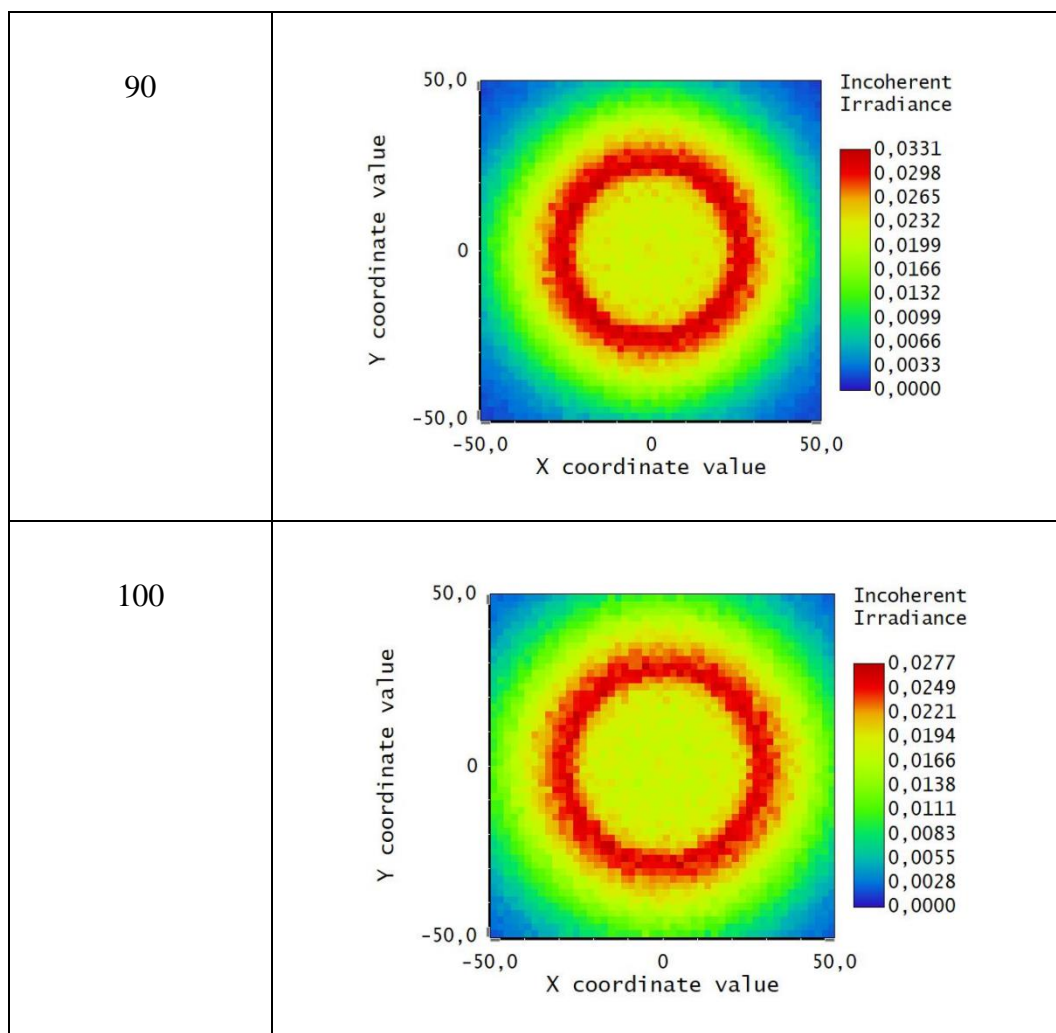
(Ts=25°C)

Part No.		NSSU123
Peak Wavelength $\lambda_p$	Typ.(nm)	375
Radiant Flux $\Phi_E$	Typ.(mW)	17.6
Forward Voltage $V_F$	Typ.(V)	3.3
	Max.(V)	4.0
Directivity $2\theta_{1/2}$	Typ.(degree)	125
$I_F$	(mA)	20
Size	LxWxH (mm)	3.0x2.0x0.7

**ANNEX 4:** Distance vs. irradiance at 365 nm.

Distance (cm)	Irradiance W/cm <sup>2</sup>
30	 <p>Incoherent Irradiance</p> <ul style="list-style-type: none"> <li>0,260</li> <li>0,234</li> <li>0,208</li> <li>0,182</li> <li>0,156</li> <li>0,130</li> <li>0,104</li> <li>0,078</li> <li>0,052</li> <li>0,026</li> <li>0,000</li> </ul>
40	 <p>Incoherent Irradiance</p> <ul style="list-style-type: none"> <li>0,152</li> <li>0,137</li> <li>0,122</li> <li>0,107</li> <li>0,091</li> <li>0,076</li> <li>0,061</li> <li>0,046</li> <li>0,030</li> <li>0,015</li> <li>0,000</li> </ul>
50	 <p>Incoherent Irradiance</p> <ul style="list-style-type: none"> <li>0,100</li> <li>0,090</li> <li>0,080</li> <li>0,070</li> <li>0,060</li> <li>0,050</li> <li>0,040</li> <li>0,030</li> <li>0,020</li> <li>0,010</li> <li>0,000</li> </ul>

<p>60</p>	 <p>Incoherent Irradiance</p> <ul style="list-style-type: none"> <li>0,0710</li> <li>0,0639</li> <li>0,0568</li> <li>0,0497</li> <li>0,0426</li> <li>0,0355</li> <li>0,0284</li> <li>0,0213</li> <li>0,0142</li> <li>0,0071</li> <li>0,0000</li> </ul>
<p>70</p>	 <p>Incoherent Irradiance</p> <ul style="list-style-type: none"> <li>0,0538</li> <li>0,0484</li> <li>0,0430</li> <li>0,0377</li> <li>0,0323</li> <li>0,0269</li> <li>0,0215</li> <li>0,0161</li> <li>0,0108</li> <li>0,0054</li> <li>0,0000</li> </ul>
<p>80</p>	 <p>Incoherent Irradiance</p> <ul style="list-style-type: none"> <li>0,0420</li> <li>0,0378</li> <li>0,0336</li> <li>0,0294</li> <li>0,0252</li> <li>0,0210</li> <li>0,0168</li> <li>0,0126</li> <li>0,0084</li> <li>0,0042</li> <li>0,0000</li> </ul>



**ANNEX 5.** Expectation and replications of the system.

